Supporting Information

Ultrabright AIEdots with Tunable Narrow Emission for Multiplexed Fluorescence Imaging

Xiaobo Zhou[#], Lingfeng Zhao[#], Ke Zhang, Chaojie Yang, Shijie Li, Xiaoxia Kang, Guo Li, Qi Wang, Haiwei Ji, Mingmin Wu, Jinxia Liu, Yuling Qin*, Li Wu**

School of Public Health, Nantong University, Nantong 226019, Jiangsu, China.
E-mail: wuli8686@ntu.edu.cn; xbzhou@ntu.edu.cn; ylqin@ntu.edu.cn

Contents

Instruments and materials

The ^{1}H and ^{13}C NMR characterization were measured at room temperature using Bruker Ultra Shield Plus 400 MHz NMR instrument. UV-Vis absorption spectra were recorded on UV1900 (Shimadzu, Japan). Photoluminescent spectra were measured using an FS5 (Edinburgh, England) system with a xenon lamp as the excitation source. Transmission electron microscopy (TEM) was conducted on a JEOL transmission electron microscope (JEM-2100) at an acceleration voltage of 100 kV. Dynamic light scattering (DLS) measurements were taken using a Malvern nanoparticle size zeta potential analyzer. Single-particle fluorescence imaging and cell imaging were carried out on a Nikon-Ti2 microscopy imaging system with a 60× immersion objective lens. The fluorescence images were collected with an EMCCD camera under an external 450 nm or 630 nm LED lamp. Lifetime studies were performed with an Edinburgh FL920 photocounting system with a semiconductor laser as the excitation source.

All chemicals were purchased from commercial sources and used without further purification. All solvents were purified before use. PS-PEGCOOH was purchased from Polymer Source Inc. PSMA was purchased from Sigma-Aldrich. The narrow emissive dye PcSi and amine-modified streptavidin were purchased from Sigma-Aldrich. Amine-modified DNA was obtained from Sangon Biotech.

Synthesis of AIEgens and narrow emissive dyes

The AIEgens TPE-BT and TPA-BT, and narrow emissive PFBDP and SQ were synthesized according to the previous report.[1-4] Their chemical structure were characterized via ^{1}H NMR and ^{13}C NMR (shown in the end of Supplementary Information).

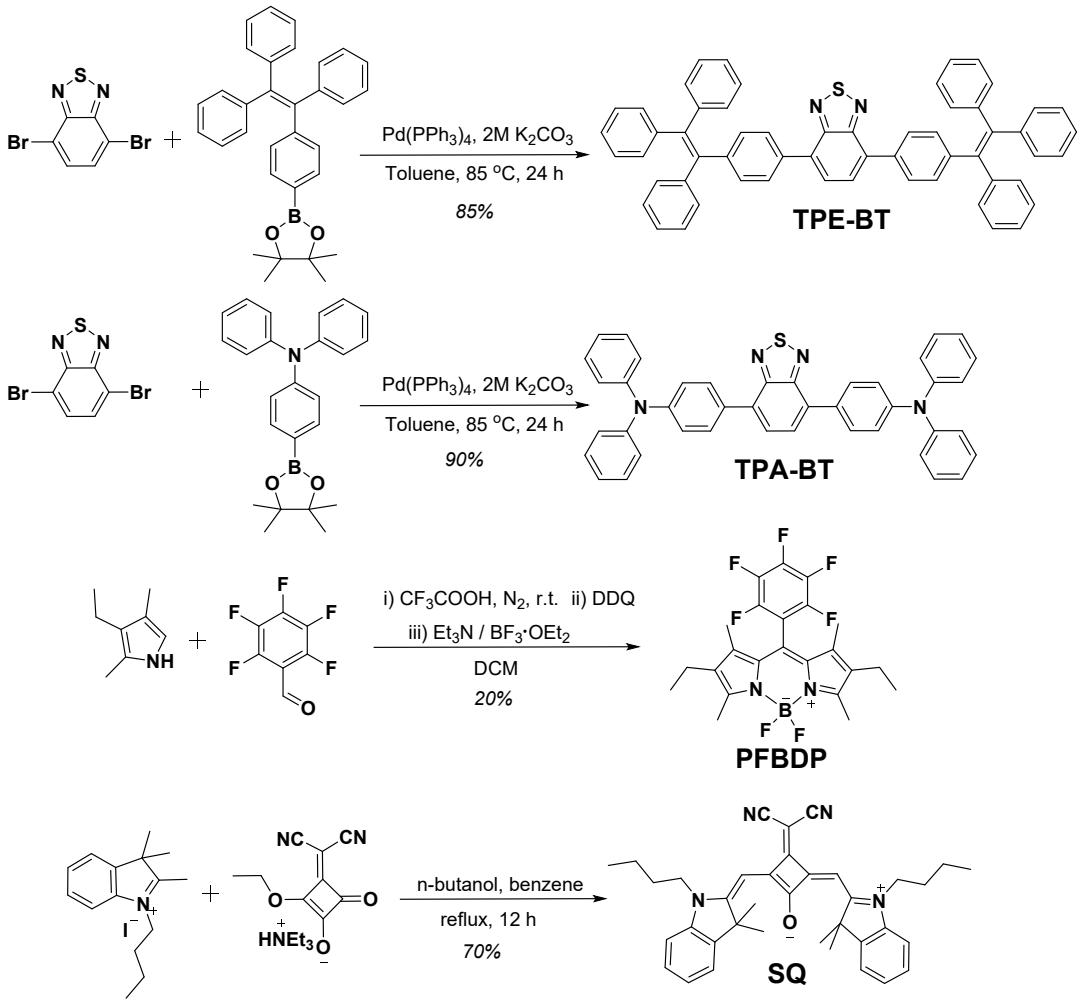

Scheme S1. Synthetic routes of TPE-BT, TPA-BT, PFBDP and SQ.

Preparation of AIEdots and NE-AIEdots

A mixture of AIEgens (0.4 mg), corresponding molar contents of narrow emissive dyes, PS-PEGCOOH (0.1 mg) and THF (0.5 mL) was sonicated to obtain a clear solution. The mixture was quickly injected into DI water (5 mL), stirring in a fume hood for 2 h and concentrating under a vacuum. Then, the solution was filtered through a membrane filter (diameter = 0.22 μm) to obtain the AIEdots. The prepared AIEdots and NE-AIEdots were stored at 4 °C for further usage.

Preparation of PFBDP NPs, SQ NPs and PcSi NPs

A mixture of narrow emissive dyes (with a content same to the dye-contents in NE-AIEdots), polystyrene (0.4 mg), PS-PEGCOOH (0.1 mg) or PSMA (0.1 mg), and THF (0.5 mL) was sonicated to obtain a clear solution. The mixture was quickly injected into DI water (5 mL), stirring in a fume hood for 2 h and concentrating under a vacuum. Then, the solution was filtered through a membrane filter (diameter = 0.22 μm) to obtain the narrow emissive dye-doped nanoparticles. The prepared nanoparticles were stored at 4 ^{o}C for further usage.

Bioconjugation of NE-AIEdots

The obtained NE-AIEdots (0.2 mg) were dispersed in 5 mL of HEPES buffer (pH = 8.4), followed by adding 2.5 mg of Triton-100 and 0.4 mg of EDC into the above solution. The suspension was stirred for another 15 min. Then, 0.25 mg of streptavidin or amine-modified DNA (20 μM, 100 μL) were injected and incubated overnight. The obtained solution was applied to the gel filtration system using Sephacry HR-300 gel media to purify the streptavidin or DNA modified NE-AIEdots. The above obtained bioconjugated NE-AIEdots solutions were stored at 4 ^{o}C for further usage.

Fluorescence quantum yield measurement

To measure the quantum yield of AIEdots, TPE-BT and TPA-BT, the reference fluorophore is fluorescien dissolved in pH 7.4 PBS (QY = 85%), Ex = 450 nm. To measure the quantum yield of PFBDP, the reference fluorophore is Rhodamine B dispersed in ethanol (QY = 65%), Ex = 500 nm. To measure the quantum yield of SQ, the reference fluorophore is Rhodamine 800 dissolved in ethanol (QY = 21%), Ex = 640 nm. To measure the quantum yield of PcSi, the reference fluorophore is ICG in DMSO (QY = 13%), Ex = 730 nm. The quantum yield was calculated in the following manner.

$$\Phi = \Phi_{ref} \times \left(n_{sample}^{2}/n_{ref}^{2}\right)\left(I_{sample}/A_{sample}\right)\left(A_{ref}/I_{ref}\right) \qquad (1)$$

Difference concentrations at or below OD 0.1 were measured and the integrated fluorescence was plotted against absorbance for every fluorescent molecular. Comparison of the slopes led to the determination of the quantum yield of fluorophore.

Calculations on the Förster radius

The parameters of the AIEgens and narrow emissive dyes were obtained from measurements in toluene solutions. The Förster radius (R_0) of different donor-acceptor pairs was calculated according to the following equation (2).

$$R_0^6 = 8.79 \times 10^{-25} \times k^2 n^{-4} \Phi_D J_{DA} \qquad (2)$$

$$J_{DA} = \frac{\int_0^\infty \varepsilon(\lambda) \cdot I(\lambda) \cdot \lambda^4 d\lambda}{\int_0^\infty I(\lambda) d\lambda} \qquad (3)$$

Where k^2 is the dipolar interaction orientation factor average to a value of 2/3. n is the refractive index of the medium (for toluene, n is 1.496). Φ_D is the quantum yield of the donor. J_{DA} is the overlap integral of the donor-acceptor pair which is determined from the recorded absorption spectrum of the acceptor (ε(λ)) and emission spectra of the donor (I(λ)) according to the equation (3).

Calculations of quenching efficiency and energy transfer (ET) efficiency

We examined the quenching efficiency using the following Stern-Volmer equation (4). Where F_0 and F represent the fluorescence intensity of the donor without and with the acceptor, respectively. The value [A] stands for the concentration of the acceptor, and K_{SV} is the Stern-Volmer quenching constant. The ET efficiency was examined by using the following equation (5).

$$F_0/F = 1 + K_{SV}[A] \qquad (4)$$

$$ET\ efficiency = 1 - F/F_0 \qquad (5)$$

Evaluation of photosensitized singlet oxygen ($^1O_2$)

The photosensitized singlet oxygen ($^1O_2$) capacity of AIEdots was tested by using 9,10-Anthracenediyl-bis(methylene) dimalonicacid (ADMA) as the $^1O_2$ indicator. The experiment was conducted by mixing AIEdots (20 μg/mL) or HP (30 μM) in aqueous solution with ADMA (50 μM). The absorption spectra were recorded after 5 minutes irradiation under the same excitation condition as for fluorescence imaging (xenon lamp, equipped with 500 nm short-pass optical filter).

Single-particle brightness measurement

For measuring the brightness of a single particle, the AIEdots and commercial QDs were diluted in glycerine and oleic acid, respectively. The fluorescence imaging process was performed on a customized wide-field epifluorescence microscope (Nikon-Ti2, Japan). The excitation light source used in microscopic fluorescence imaging was a high-power xenon lamp (300 W, Sutter instrument-Lambda LS, USA), equipped with bandpass or short-pass filters with different cut-off wavelength. The objective for illumination and light collection was a Nikon CFI Plan Apochromat Lambda 60× objective lens with 60× magnification and 1.40 NA. The fluorescence signal was collected from different channels with an sCMOS camera (Hamamatsu Flash4.0 LT+, Japan) by using different long-pass filters (495LP: 495 nm long-pass filter, 600LP: 600 nm long-pass filter) and bandpass filters (550BP: 520-580 nm bandpass filter, 630BP: 600-660 nm bandpass filter, 732BP: 700-765 nm bandpass filter, 792BP: 760-824 nm bandpass filter). Fluorescence intensity emitted per frame for a given particle was estimated by integrating the sCMOS signal over the fluorescent spot.

Cytotoxicity test

The *in vitro* cytotoxicity was measured using a standard methyl thiazolyl tetrazolium (MTT, Sigma Aldrich) assay in HeLa cell lines. Briefly, cells growing in log phase were seeded into 96-well cell culture plate at 1×10^4/well. TPEdots, TPAdots, PFdots, SQdots and PcSidots was added to the wells of the treatment group at concentrations of 0, 1.25, 2.5, 5, 10, 20, 40, 80, 120 μg/mL. For the negative control group, 1 μL/well solvent was diluted in DMEM with the

final concentration of 1 %. The cells were incubated for 24 h and 48 h at 37 °C under 5 % CO_2. The combined MTT/PBS solution was added to each well of the 96-well assay plate and incubated for an additional 4 h. After removal of the culture solution, 200 μL DMSO was added to each well, shaking for 10 min at shaking table. An enzyme-linked immunosorbent assay (ELISA) reader was used to measure the OD570 (absorbance value) of each well referenced at 490 nm. The following formula was used to calculate the viability of cell growth: Viability (%) = (mean of absorbance value of treatment group / mean of absorbance value of control) × 100

Cell culture and imaging

Human serous cancer cell line HeLa were provided by the Institute of Biochemistry and Cell Biology, SIBS, CAS (China). HeLa cells were grown in DMEM supplemented with 10% FBS (fetal bovine serum) at 37 ºC and 5% CO_2. The cells were planted on 14 mm glass coverslips and keep to adhere for 24 h. For fluorescence imaging of living cells with the AIEdots, NE-AIEdots, NE-AIEdots-SA and NE-AIEdots-DNA, the cells were incubated with these nanoprobes at a concentration of 20 μg/mL, under the condition of 37 ºC, 5% CO_2 for 12 h, then washed with phosphate-buffered saline (PBS) three times. For the nuclear staining experiments, DAPI probe was added 1h before fluorescence imaging. Then the fluorescence signal was recorded using DAPI channel (Ex: 379/34BP, Em: 452/40BP). The fluorescence signal of TPAdots was collected with the other channel (Ex: 500SP, Em: 600LP).

Fluorescence imaging in vitro and in vivo

The *in vivo* and *in vitro* fluorescence imaging were performed by using the homemade imaging system fabricated by ourselves. Animal experiments were conducted according to the guidelines of the Institutional Animal Care and Use Committee, Laboratory Animal Center, Nantong University. The luminescent signals from AIEdots were collected using an EMCCD camera. The system was equipped with different long-pass filters (495LP, 600LP) and bandpass filters (550BP, 630BP, 732BP and 792BP) for collecting fluorescence signals of

different AIEdots in different collection channels. The excitation source for *in vitro* and *in vivo* experiments was a 450 nm LED lamp. For fluorescence imaging *in vivo*, the nude mice (n = 3) were separately subcutaneous injected with PFdots, SQdots, PcSidots and MNE-AIEdots to different footpads with a total dose of 0.5 mg/mL (25 μL). The average signal of solutions and tissues was analyzed by the Bruker imaging software and Origin 8.0 software.

Histological analysis

After fluorescence imaging *in vivo*, the lymph node tissues were harvested and fixed in 4% paraformaldehyde for H&E staining analysis, embedded in paraffin, sectioned and stained with hematoxylin and eosin. The sections were observed under an optical microscope.

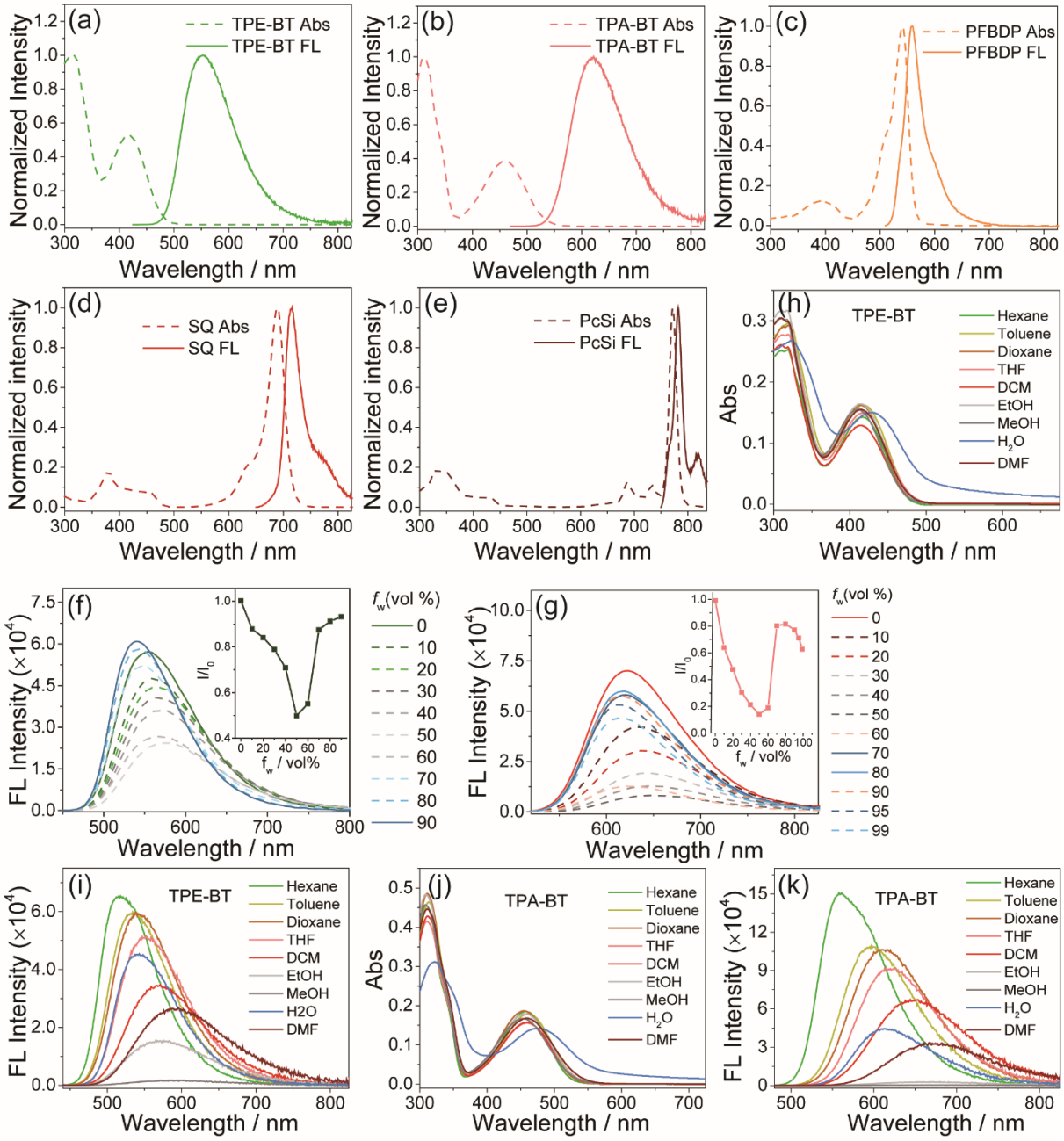

Figure S1. Normalized absorption (dash line) and fluorescence (solid line) spectra of TPE-BT (a), TPA-BT (b), PFBDP (c), SQ (d) and PcSi (e) in tetrahydrofuran (THF). Fluorescence spectra of TPE-BT (f) and TPA-BT (g) in different water fractions (f_w vol%). Inset: corresponding plots of AIE curves of TPE-BT and TPA-BT in the different water fractions (vol%). Absorption and fluorescence spectra of TPE-BT (h, i) and TPA-BT (j, k) measured in different solvent.

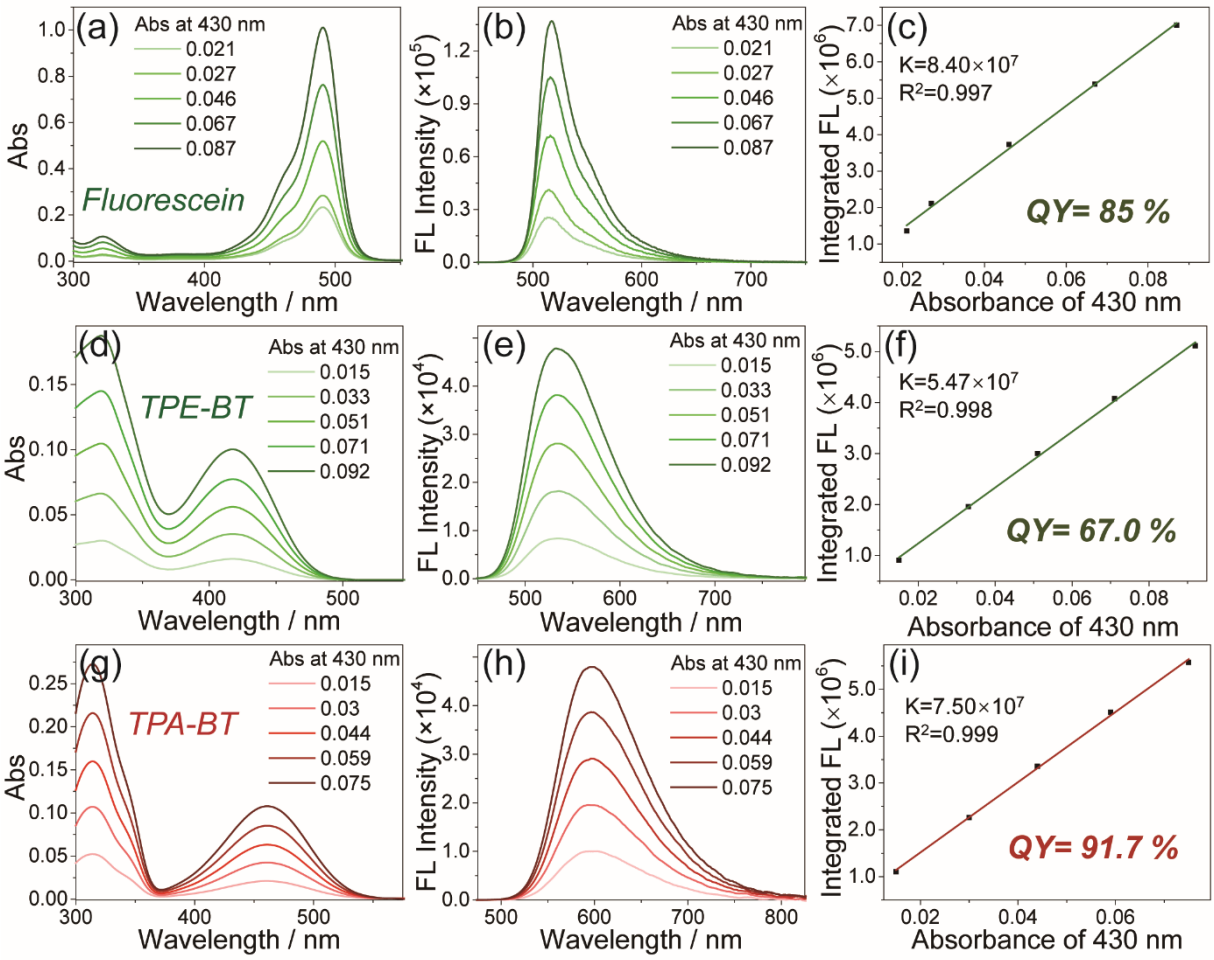

Figure S2. Fluorescence quantum yield measurement of TPE-BT and TPA-BT in toluene. Absorption spectra of different concentrations of reference compound (fluorescien, in pH 7.4 PBS, QY = 0.85, a), TPE-BT (d) and TPA-BT (g) in toluene. Corresponding fluorescence spectra of different concentrations of fluorescien (b), TPE-BT (e) and TPA-BT (h), respectively. Excitation: 430 nm. (c) Integrated fluorescence intensity plotted as a function of absorbance at 430 nm for fluorescien solutions based on the measurements in a) and b). The data was fitted into a linear function with a slope of 8.40×10^7. (f) Integrated fluorescence intensity plotted as a function of absorbance at 430 nm for TPE-BT solutions based on the measurements in d) and e). The data was fitted into a linear function with a slope of 5.47×10^7. (i) Integrated fluorescence intensity plotted as a function of absorbance at 430 nm for TPA-BT solutions based on the measurements in g) and h). The data was fitted into a linear function with a slope of 7.50×10^7.

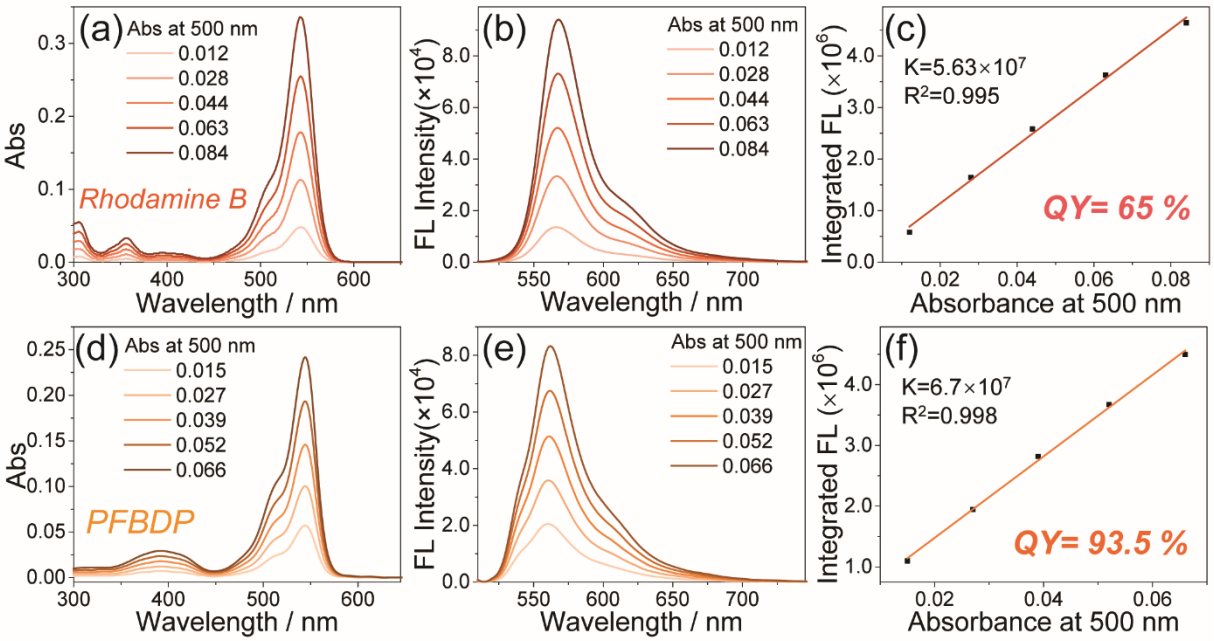

Figure S3. Fluorescence quantum yield measurement of PFBDP in toluene. Absorption spectra of different concentrations of reference compound (Rhodamine B, in ethanol, QY = 0.65, a), and PFBDP (in toluene, d). Corresponding fluorescence spectra of different concentrations of Rhodamine B (b) and PFBDP (e), respectively. Excitation: 500 nm. (c) Integrated fluorescence intensity plotted as a function of absorbance at 500 nm for Rhodamine B solutions based on the measurements in a) and b). The data was fitted into a linear function with a slope of 5.63×10^7. (f) Integrated fluorescence intensity plotted as a function of absorbance at 515 nm for PFBDP solutions based on the measurements in d) and e). The data was fitted into a linear function with a slope of 6.7×10^7.

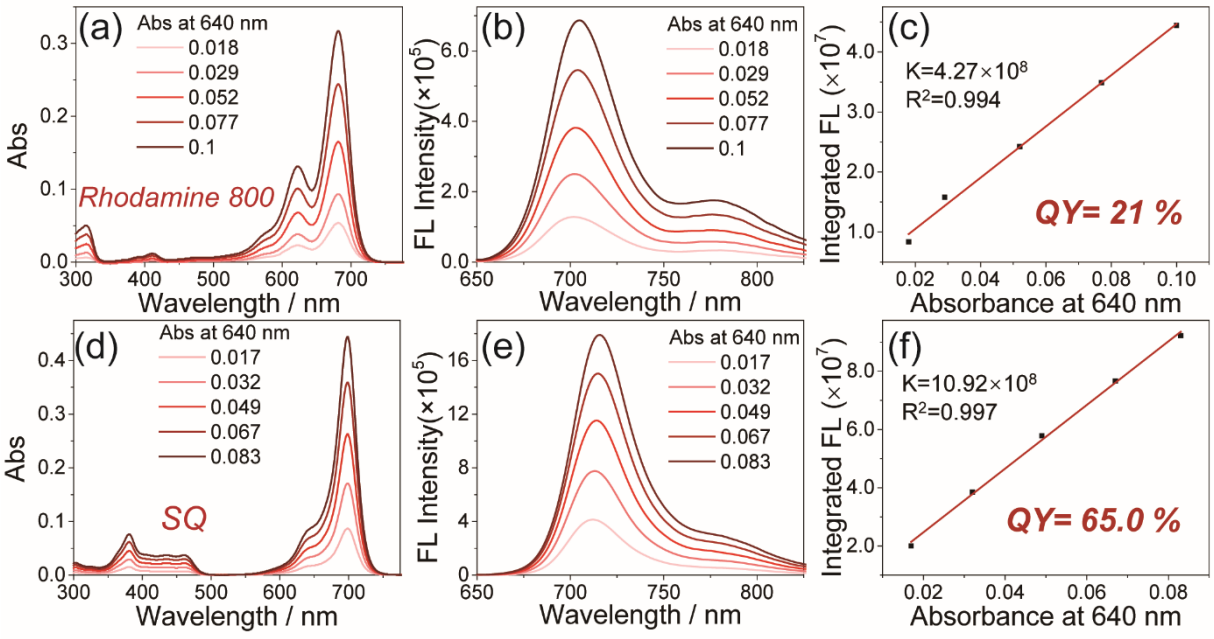

Figure S4. Fluorescence quantum yield measurement of SQ in toluene. Absorption spectra of different concentrations of reference compound (Rhodamine 800, in ethanol, QY = 0.21, a) and SQ (d, in toluene). Corresponding fluorescence spectra of different concentrations of Rhodamine 800 (b) and SQ (e), respectively. Excitation: 640 nm. (c) Integrated fluorescence intensity plotted as a function of absorbance at 640 nm for Rhodamine 800 solutions based on the measurements in a) and b). The data was fitted into a linear function with a slope of 4.27×10^8. (f) Integrated fluorescence intensity plotted as a function of absorbance at 640 nm for SQ solutions based on the measurements in d) and e). The data was fitted into a linear function with a slope of 10.92×10^8.

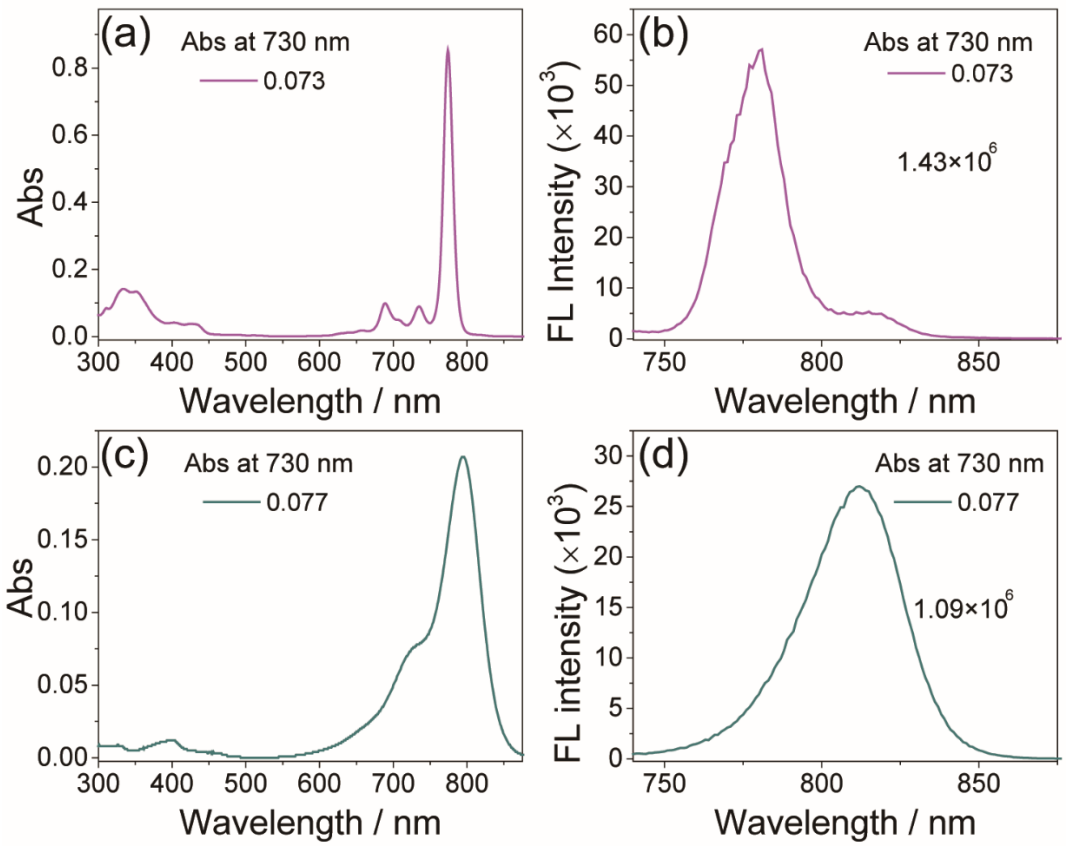

Figure S5. Fluorescence quantum yield measurement of PcSi in toluene. Absorption spectra of ICG (in DMSO, QY = 0.13, a) and PcSi (in toluene, c). Corresponding fluorescence spectra of ICG (b) and PcSi (d), respectively. Excitation: 730 nm. Integrated fluorescence intensity of ICG and PcSi were separately calculated to be 1.09×10^6 and 1.43×10^6.

Table S1. Photophysical characterization of TPE-BT, TPA-BT, PFBDP, SQ and PcSi in toluene.

Fluorophores	$\lambda_{max, abs}$ [nm]	ε ($\lambda_{max, abs}$) [$M^{-1}cm^{-1}$]	$\lambda_{max, em}$ [nm]	Φ [%]	Brightness ($\varepsilon \times \Phi \times N_A$)	Stokes shift [nm]	$FWHM_{em}$ [nm]
TPE-BT	415	25500	537	67.0[a]	17100	122	96
TPA-BT	460	21500	600	91.7[a]	19800	140	104
PFBDP	545	28600	562	93.7[b]	26900	17	40
SQ	700	239100	715	65.0[c]	155400	15	37
PcSi	772	432700	783	18.4[d]	79600	11	16

Φ is the relative fluorescence quantum yield estimated by using a) Fluorescein (Φ = 0.85, in pH 7.4 PBS) as a reference fluorophore, Exitation-430 nm, b) Rhodamine B (Φ = 0.65, in ethanol) as a reference fluorophore, Exitation-500 nm, c) Rhodamine 800 (Φ = 0.21, in ethanol) as a reference fluorophore, Exitation-640 nm, d) ICG (Φ = 0.13, in DMSO) as a reference fluorophore, Exitation-730 nm. $FWHM_{em}$-the full width at half-maximum of the emission band of fluorophore.

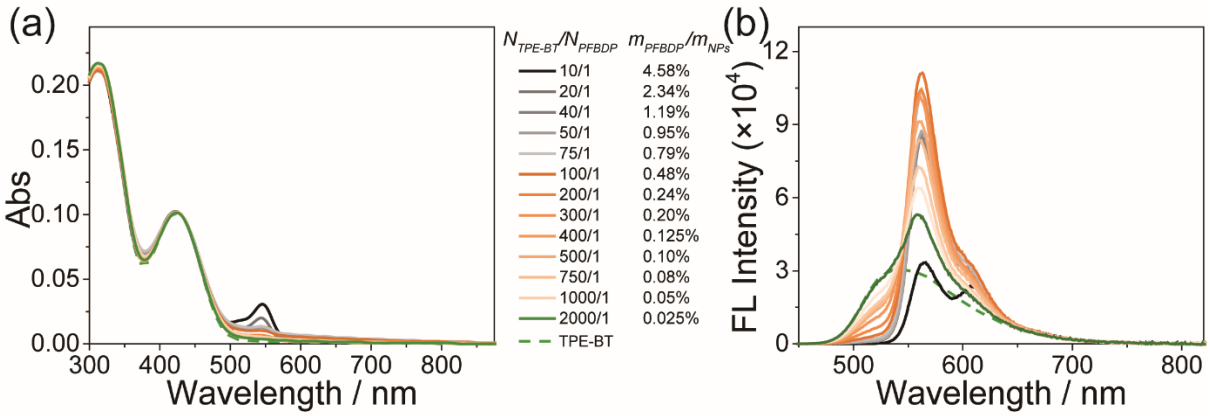

Figure S6. Absorption (a) and emission (b) spectra of the prepared AIEdots, which consist of TPE-BT (mass fraction, 80%), PFBDP (mass fraction, range from 0-4.58%) and PS-PEGCOOH. The molar ratio of TPE-BT to PFBDP ranges from 2000/1 to 10/1.

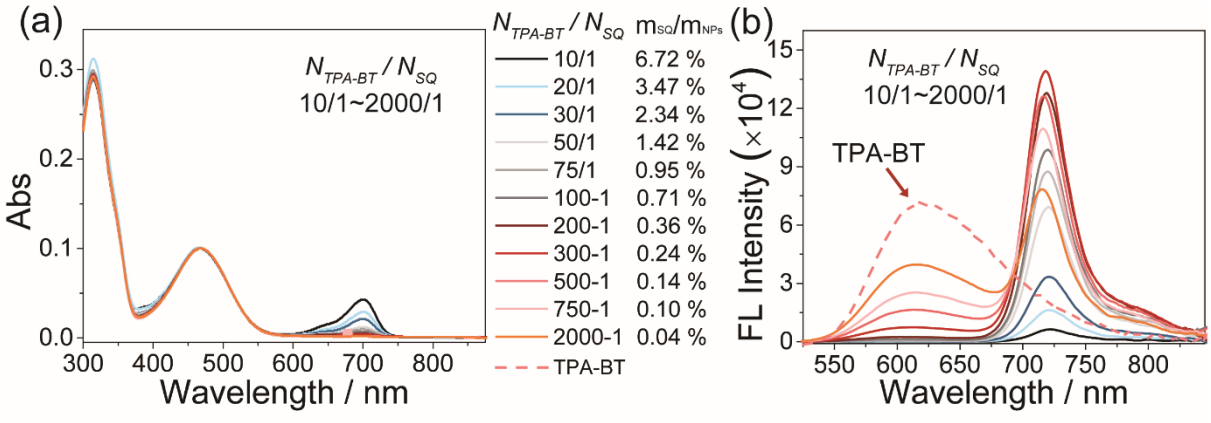

Figure S7. Absorption (a) and emission (b) spectra of the prepared AIEdots, which consist of TPA-BT (mass fraction, 80%), SQ (mass fraction, range from 0%-6.72%) and PS-PEGCOOH. The molar ratio of TPA-BT to SQ ranges from 2000/1 to 10/1.

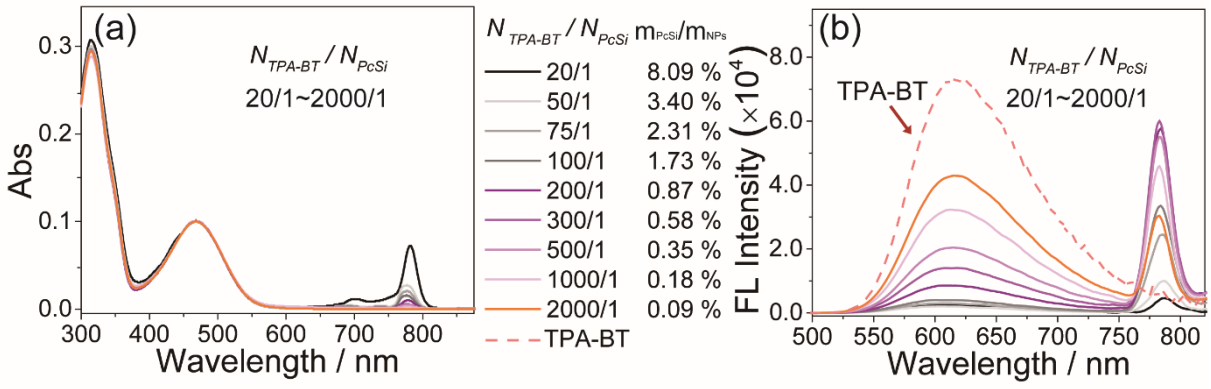

Figure S8. Absorption (a) and emission (b) spectra of the prepared AIEdots, which consist of TPA-BT (mass fraction, 80%), PcSi (mass fraction, range from 0%-8.09%) and PS-PEGCOOH. The molar ratio of TPA-BT to PcSi ranges from 2000/1 to 20/1.

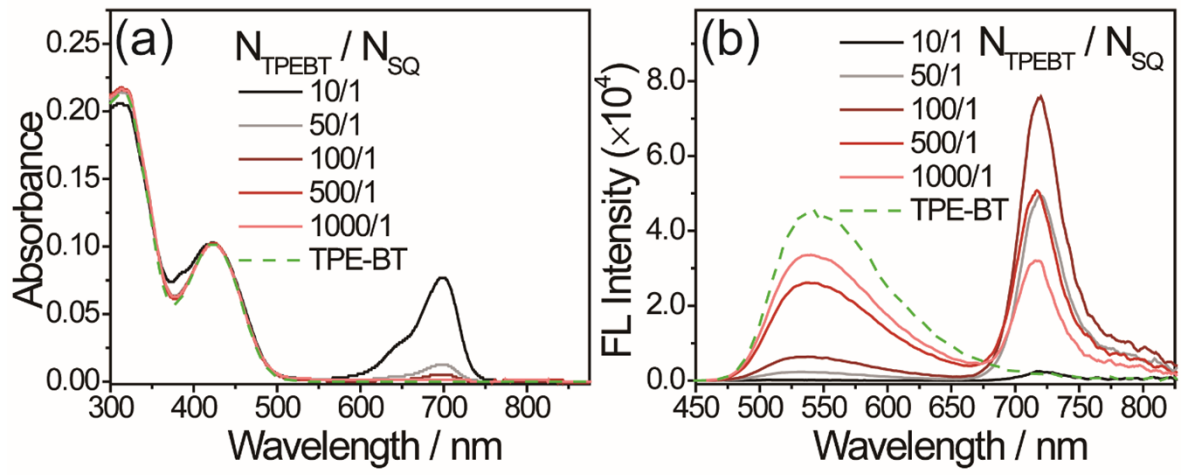

Figure S9. Absorption (a) and emission (b) spectra of the prepared AIEdots, which consist of TPE-BT (mass fraction, 80%), SQ (mass fraction, range from 0.09%-8.09%) and PS-PEGCOOH. The molar ratio of TPE-BT to PcSi ranges from 1000/1 to 10/1.

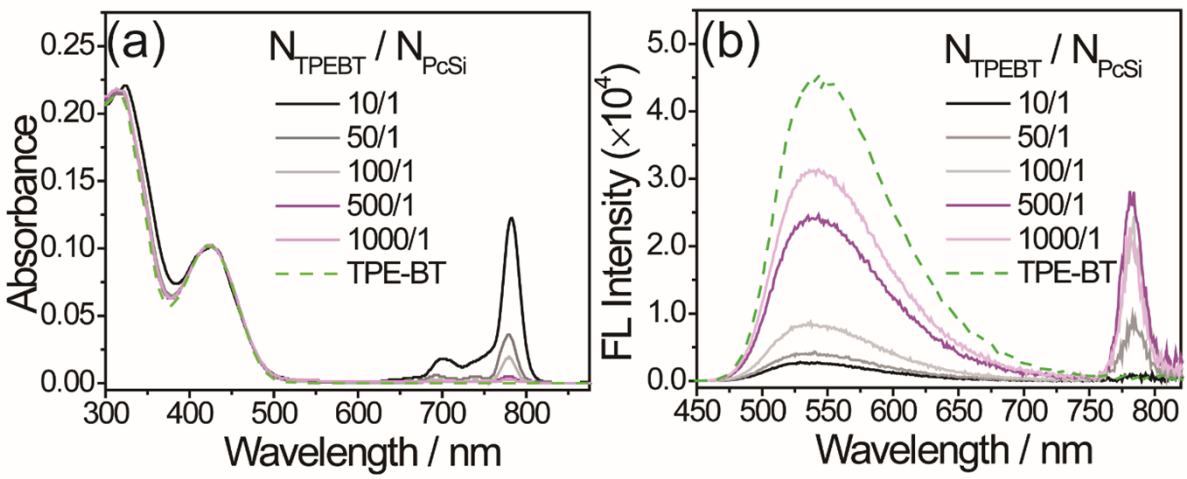

Figure S10. Absorption (a) and emission (b) spectra of the prepared AIEdots, which consist of TPE-BT (mass fraction, 80%), PcSi (mass fraction, range from 0.09%-8.09%) and PS-PEGCOOH. The molar ratio of TPE-BT to PcSi ranges from 1000/1 to 10/1.

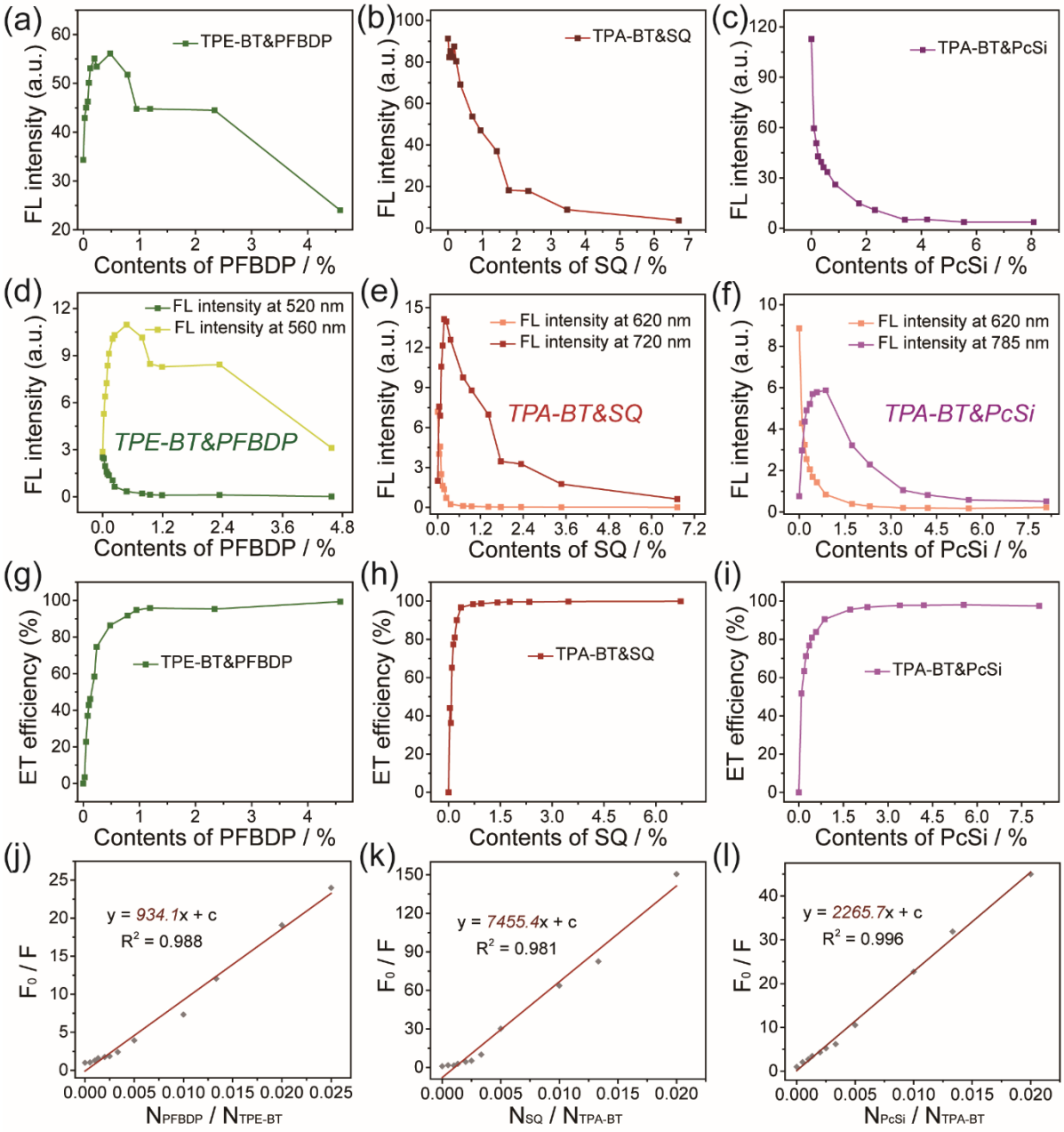

Figure S11. (a-c) Relationships between the integrated fluorescence intensity of the donor&acceptor codoped AIEdots (a, TPE-BT&PFBDP; b TPA-BT&SQ; c, TPA-BT&PcSi) and the contents of doped acceptors. (d) Relationships between the fluorescence intensity of TPE-BT&PFBDP co-doped AIEdots at 520 nm and 560 nm and the contents of PFBDP respectively. (e) Relationships between the fluorescence intensity of TPA-BT&SQ codoped AIEdots at 620 nm and 720 nm and the contents of SQ, respectively. (f) Relationships between the fluorescence intensity of TPA-BT&PcSi codoped AIEdots at 620 nm and 785 nm and the contents of PcSi, respectively. (g-i) Energy transfer efficiency of different AIEdots

with the varied content of acceptor. (g) Energy transfer efficiency of TPE-BT&PFBDP codoped AIEdots with the varied content of PFBDP. (h) Energy transfer efficiency of TPA-BT&SQ codoped AIEdots with the varied content of SQ. (i) Energy transfer efficiency of TPA-BT&PcSi codoped AIEdots with the varied content of PcSi. (j-l) Quenching of different AIEdots with the varied content of acceptor. (j) Quenching of TPE-BT&PFBDP codoped AIEdots with the varied content of PFBDP. (h) Quenching of TPA-BT&SQ codoped AIEdots with the varied content of SQ. (i) Quenching of TPA-BT&PcSi codoped AIEdots with the varied content of PcSi.

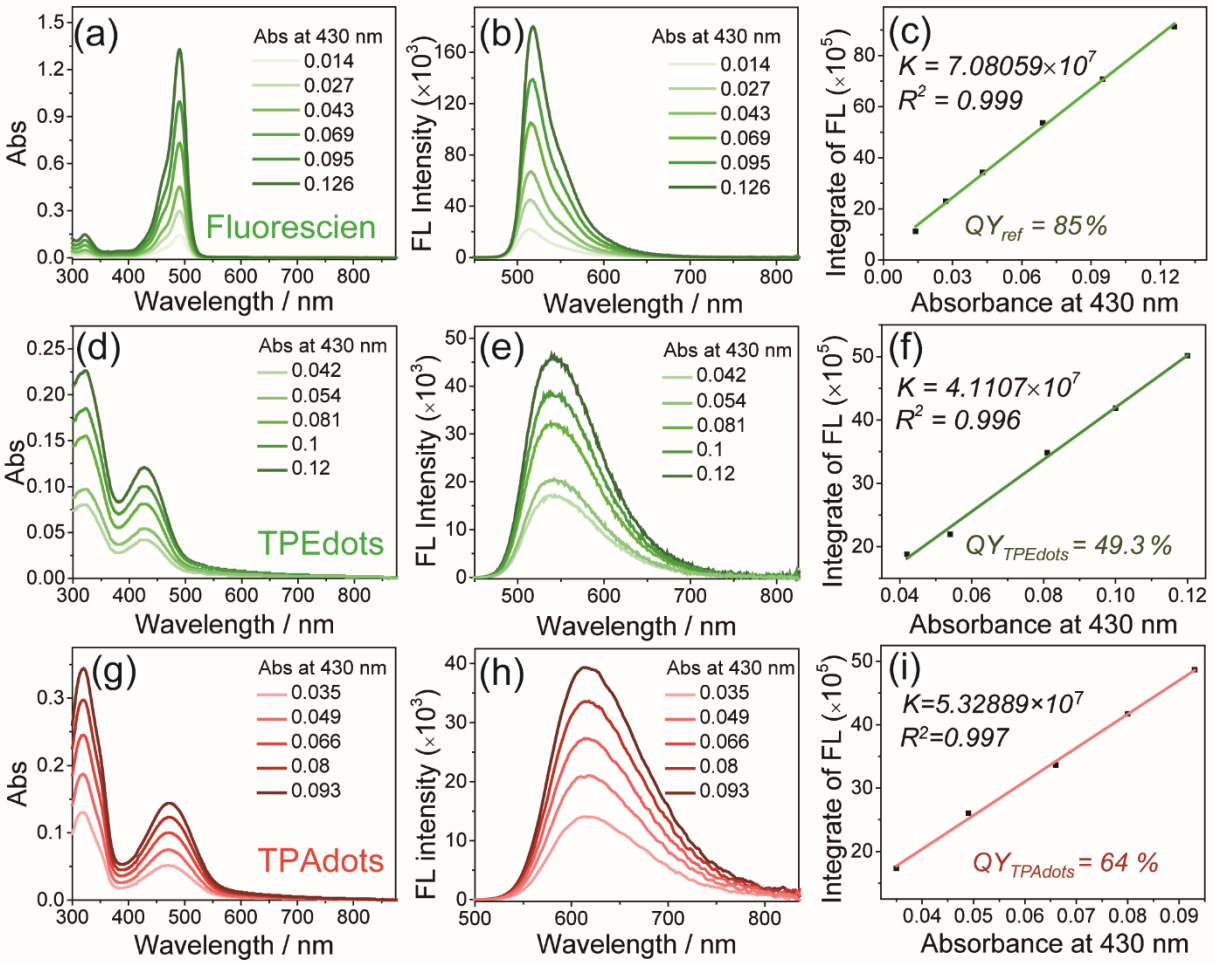

Figure S12. Fluorescence quantum yield measurement of TPEdots and TPAdots in water. Absorption spectra of different concentrations of reference compound (fluorescien, in pH 7.4 PBS, QY = 0.85, a), TPEdots (in water, d) and TPAdots (in water, g). Corresponding fluorescence spectra of different concentrations of fluorescien (b), TPEdots (e) and TPAdots (h) respectively. Excitation: 430 nm. (c) Integrated fluorescence intensity plotted as a function of absorbance at 430 nm for fluorescien solutions based on the measurements in a) and b). The data was fitted into a linear function with a slope of 7.08×10^7. (f) Integrated fluorescence intensity plotted as a function of absorbance at 430 nm for TPEdots solutions based on the measurements in d) and e). The data was fitted into a linear function with a slope of 4.11×10^7. (i) Integrated fluorescence intensity plotted as a function of absorbance at 430 nm for TPAdots solutions based on the measurements in g) and h). The data was fitted into a linear function with a slope of 5.33×10^7.

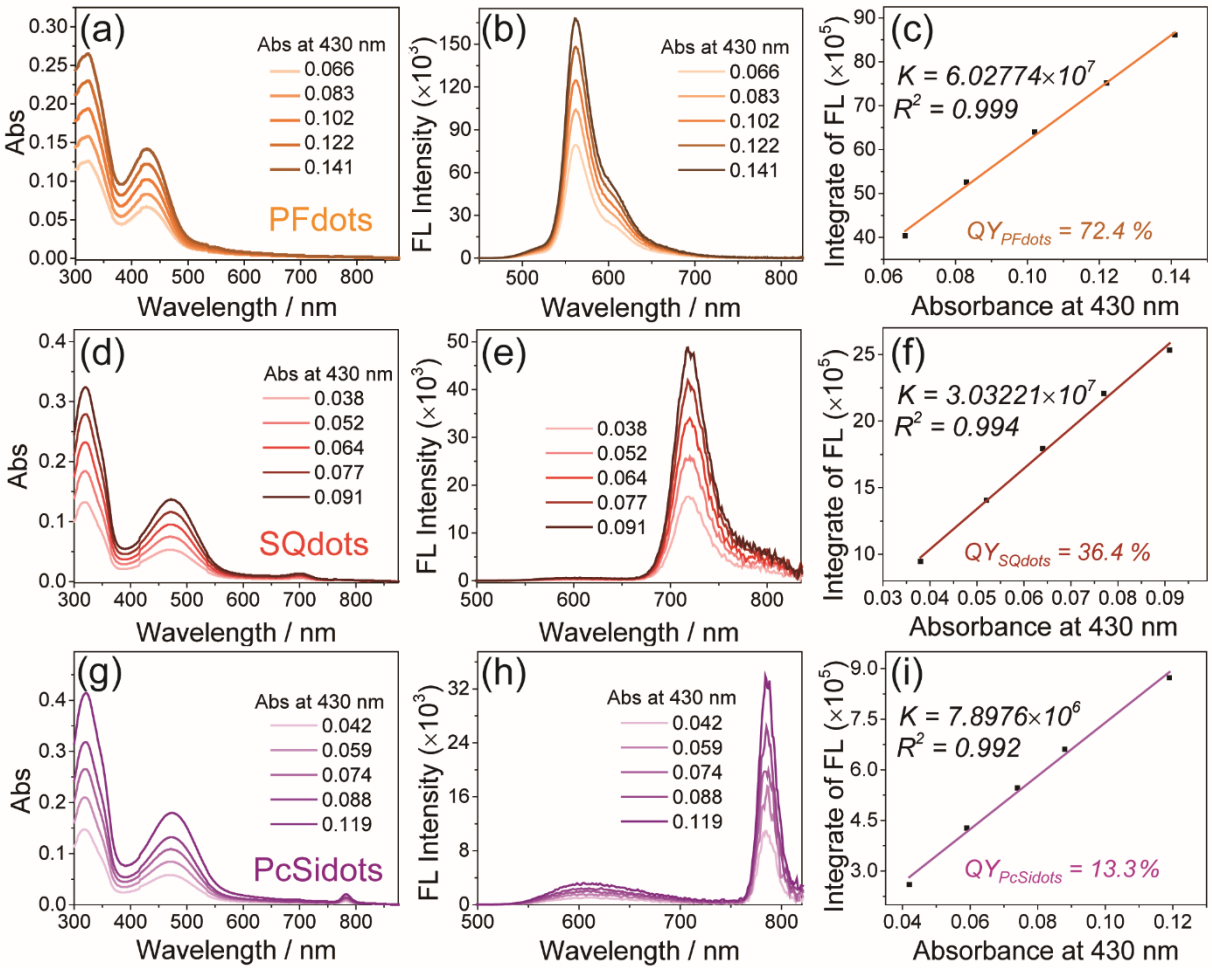

Figure S13. Fluorescence quantum yield measurement of PFdots, SQdots and PcSidots in water. Absorption spectra of different concentrations of PFdots (in water, a), SQdots (in water, d) and PcSidots (in water, g). Corresponding fluorescence spectra of different concentrations of PFdots (b), SQdots (e) and PcSidots (h), respectively. Excitation: 430 nm. (c) Integrated fluorescence intensity plotted as a function of absorbance at 430 nm for PFdots solutions based on the measurements in a) and b). The data was fitted into a linear function with a slope of 6.03×10^7. (f) Integrated fluorescence intensity plotted as a function of absorbance at 430 nm for SQdots solutions based on the measurements in d) and e). The data was fitted into a linear function with a slope of 3.03×10^7. (i) Integrated fluorescence intensity plotted as a function of absorbance at 430 nm for PcSidots solutions based on the measurements in g) and h). The data was fitted into a linear function with a slope of 0.79×10^7.

Table S2. Photophysical characterization of TPEdots, TPAdots, PFdots, SQdots and PcSidots in water.

Fluorophores	$\lambda_{max,\ abs}$ [nm]	ε_m ($\lambda_{max,\ abs}$)[a] [$Lg^{-1}cm^{-1}$]	ε ($\lambda_{max,\ abs}$)[b] [$M^{-1}cm^{-1}$]	$\lambda_{max,\ em}$ [nm]	Φ[c] [%]	Brightness of nanodots ($\varepsilon \times \Phi \times N_A$)	Stokes shift [nm]	$FWHM_{em}$ [nm]
TPEdots	425	15.04	10.40×10^7	542	49.3	5.13×10^7	117	108
TPAdots	470	16.02	7.98×10^7	620	64.0	5.11×10^7	150	114
PFdots	425	14.95	12.72×10^7	561	72.4	9.21×10^7	136	33
SQdots	470	15.88	6.09×10^7	720	36.4	2.22×10^7	250	36
PcSidots	470	15.85	7.80×10^7	787	13.3	1.04×10^7	317	18

a) ε_m-extinction coefficient of the prepared AIEdots. b) ε is the calculated molar extinction coefficient of AIEdots, according to the following equation. c) Φ is the relative fluorescence quantum yield estimated by using Fluorescein (Φ = 0.85, in pH 7.4 PBS) as a reference fluorophore, Exitation-430 nm. $FWHM_{em}$-the full width at half-maximum height of emission band.

$$M_{AIEdots} \approx \rho V_{AIEdots} = \rho 4\pi r^3_{AIEdots}/3 \quad (1)$$

$$\varepsilon = \varepsilon_m \times M_{AIEdots} \times N_A \quad (2)$$

Where $M_{AIEdots}$ is the single particle mass of organic nanoparticle; ρ is the density of organic nanoparticles (the value of ρ is nearly to the density of water, 1.00 g/mL); $V_{AIEdots}$ is the single particle volume of organic nanoparticle; $r_{AIEdots}$ is the single particle semidiameter of organic nanoparticle (can be determined by TEM and DLS characterization, the morphology of nanoparticles are seen as sphere). N_A is the avogadro's number-6.02×10^{23}.

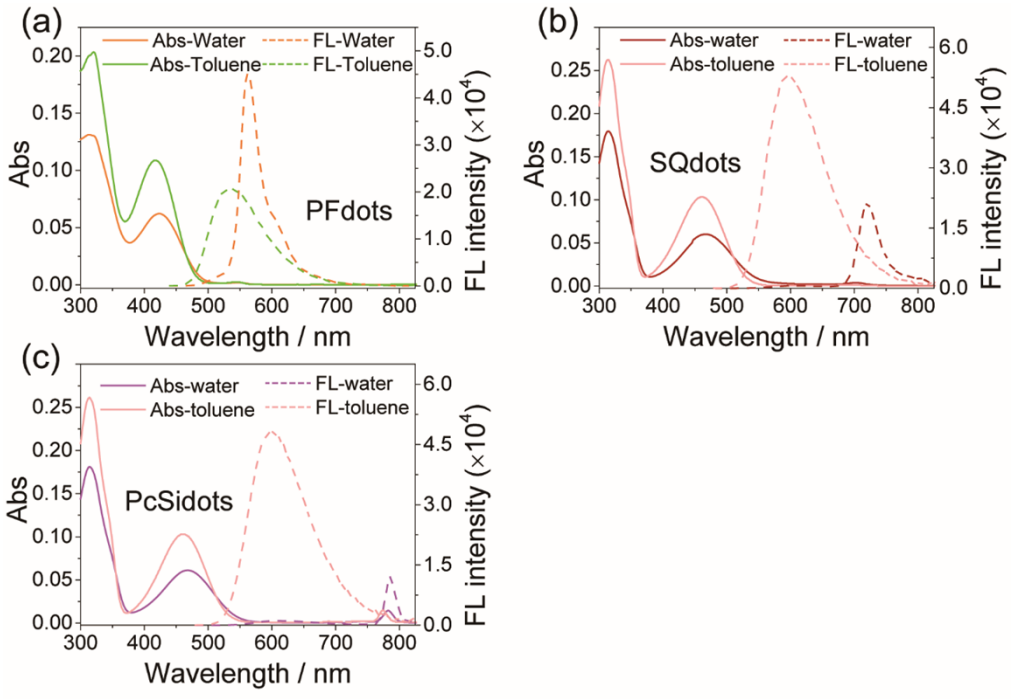

Figure S14. Absorption and fluorescence spectra of PFdots (a), SQdots (b) and PcSidots (c) in toluene and water, respectively. The measured fluorescence spectra of the NE-AIEdots in different solvents were collected under identical excitation conditions.

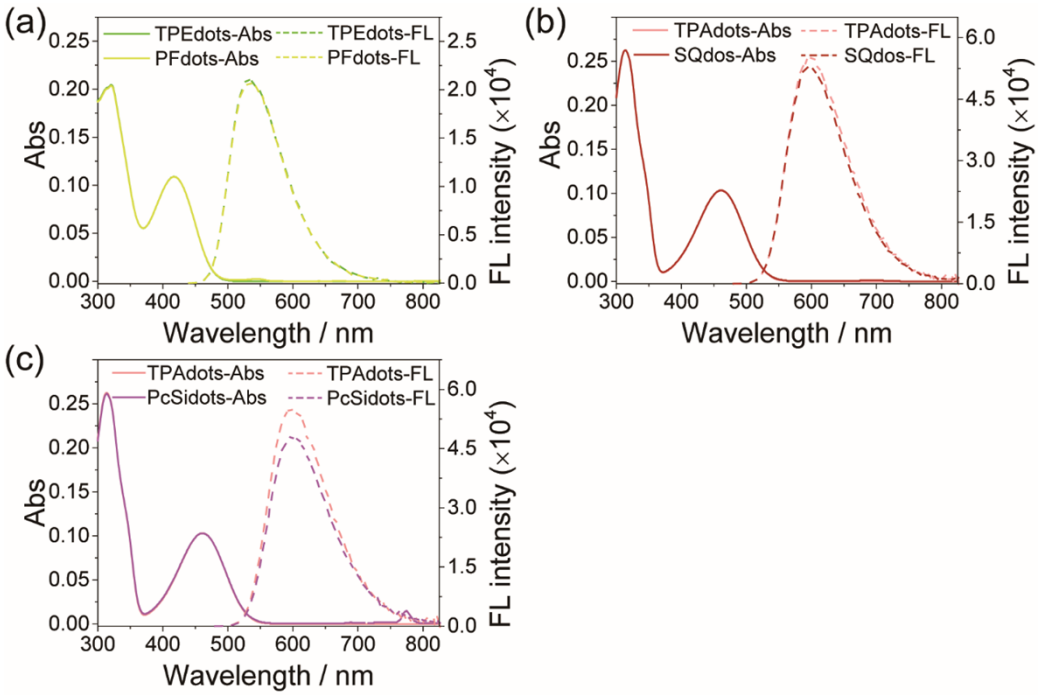

Figure S15. Absorption and fluorescence spectra of TPEdots and PFdots (a), TPAdots and SQdots (b), TPAdots and PcSidots (c) in toluene with identical concentrations.

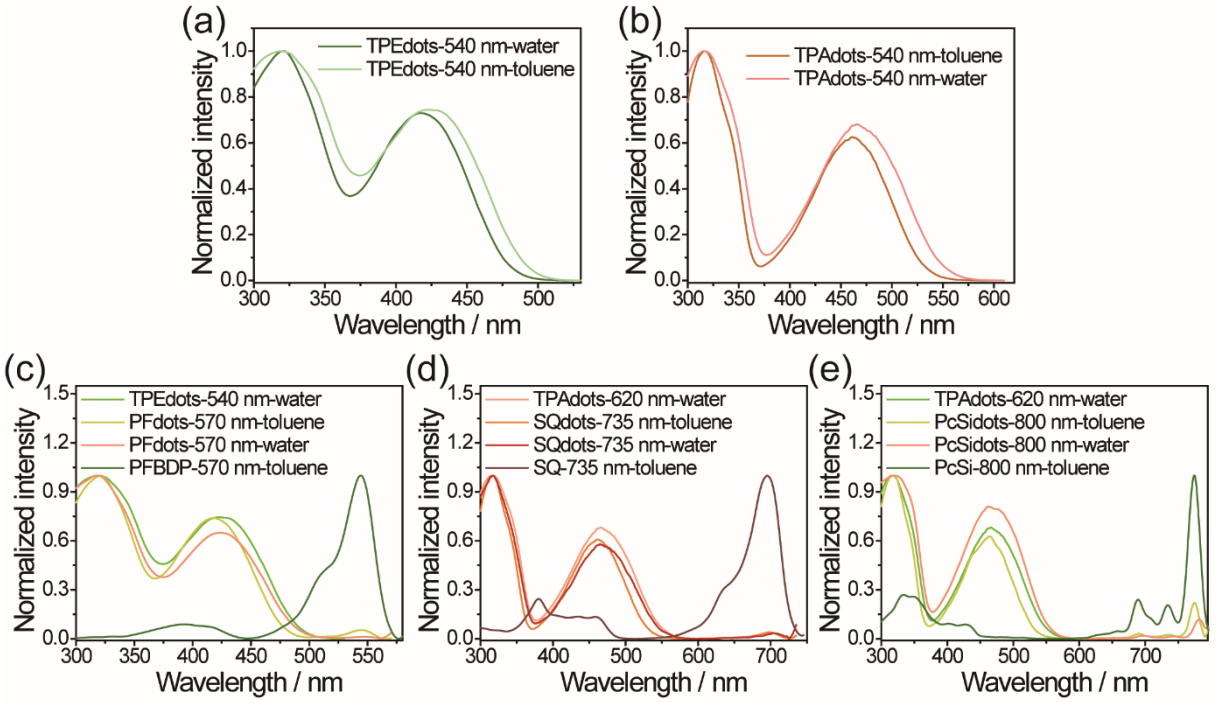

Figure S16. (a) Excitation spectra of TPEdots in water and toluene at 540 nm. (b) Excitation spectra of TPAdots in water and toluene at 620 nm. (c) Excitation spectra of TPEdots in water at 540 nm, PFdots in water at 570 nm, PFBDP and PFdots in toluene at 570 nm. (d) Excitation spectra of TPAdots in water at 620 nm, SQdots in water at 735 nm, SQ and SQdots in toluene at 735 nm. (e) Excitation spectra of TPAdots in water at 620 nm, PcSidots in water at 800 nm, PcSi and PcSidots in toluene at 800 nm.

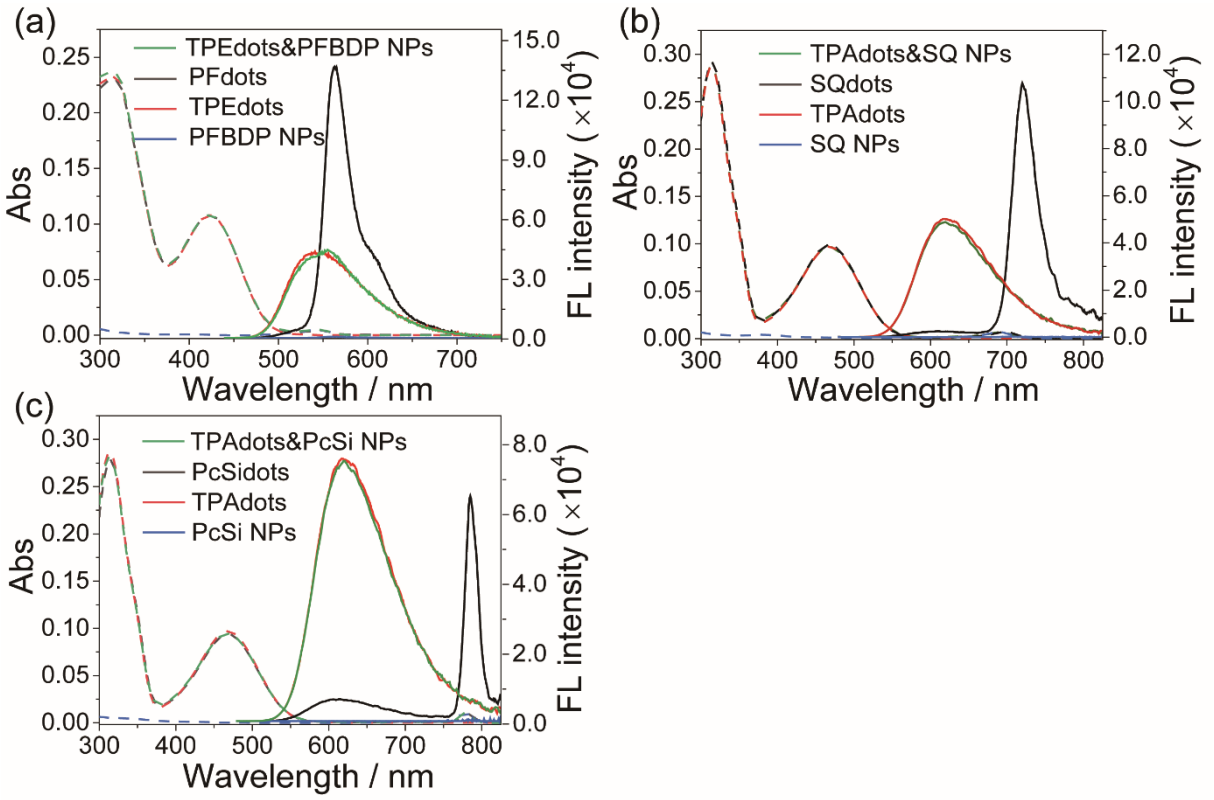

Figure S17. (a) Absorption (dash lines) and fluorescence (solid lines) spectra of PFdots, TPEdots, PFBDP NPs and TPEdots&PFBDP NPs (the mixture of TPEdots and PFBDP NPs, $N_{TPE\text{-}BT}/N_{PFBDP}$ is 100/1). Excitation: 430 nm. (b) Absorption (dash lines) and fluorescence (solid lines) spectra of SQdots, TPAdots, SQ NPs and TPAdots&SQ NPs (the mixture of TPAdots and SQ NPs, $N_{TPA\text{-}BT}/N_{SQ}$ is 200/1). Excitation: 470 nm. (c) Absorption (dash lines) and fluorescence (solid lines) spectra of PcSidots, TPAdots, PcSi NPs and TPAdots&PcSi NPs (the mixture of TPAdots and PcSi NPs, $N_{TPA\text{-}BT}/N_{PcSi}$ is 200/1). Excitation: 470 nm. The fluorophores were encapsulated in poly(styrene-co-maleic anhydride) (PSMA).

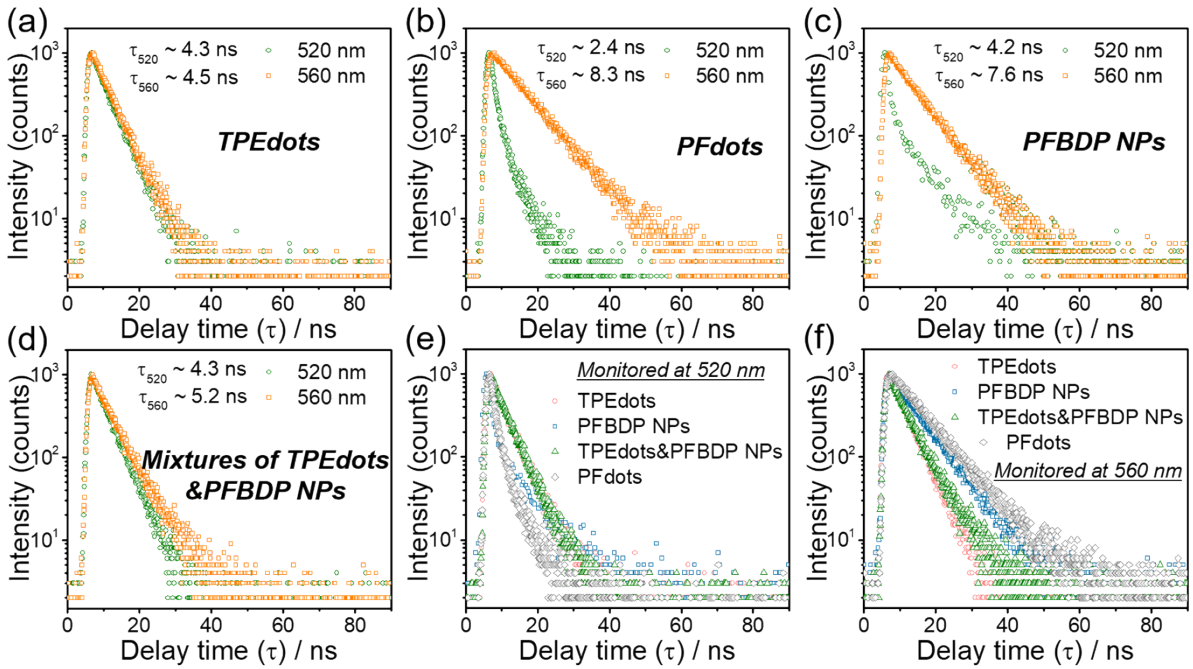

Figure S18. Fluorescence decays of TPEdots (a), PFdots (b), PFBDP NPs (c) and the mixtures of TPEdots&PFBDP NPs (d, in the mixtures, $N_{TPE\text{-}BT}/N_{PFBDP}$ = 100/1) in aqueous solution, monitored at 520 nm and 560 nm, respectively. Comparison of the fluorescence decays of TPEdots and PFdots, PFBDP NPs and TPEdots&PFBDP NPs mixtures ($N_{TPE\text{-}BT}/N_{PFBDP}$ = 100/1) monitoried at 520 nm (e) and 560 nm (f). λ_{ex} = 375 nm.

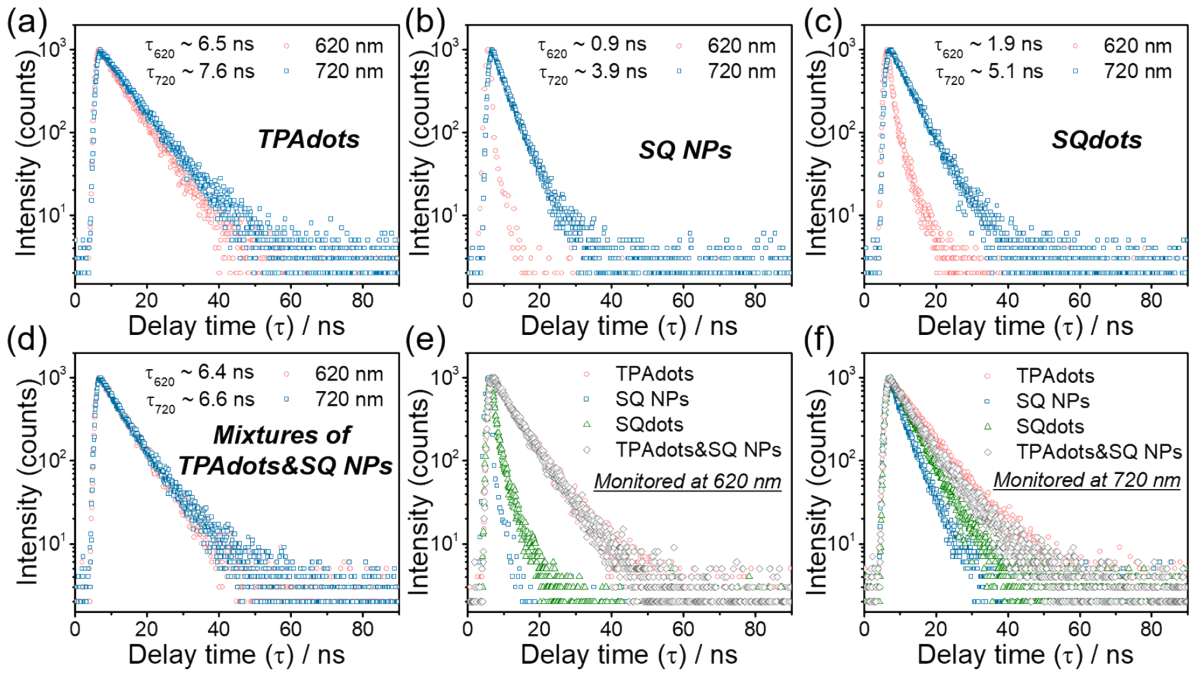

Figure S19. Fluorescence decays of TPAdots (a), SQ NPs (b), SQdots (c) and the mixtures of TPAdots&SQ NPs (d, in the mixtures, $N_{TPA\text{-}BT}/N_{SQ}$ = 200/1) in aqueous solution, monitored at 620 nm and 720 nm, respectively. Comparison of the fluorescence decays of TPAdots, SQ NPs, SQdots and TPAdots&SQ NPs mixtures ($N_{TPA\text{-}BT}/N_{SQ}$ = 200/1) monitoried at 620 nm (e) and 720 nm (f). λ_{ex} = 375 nm.

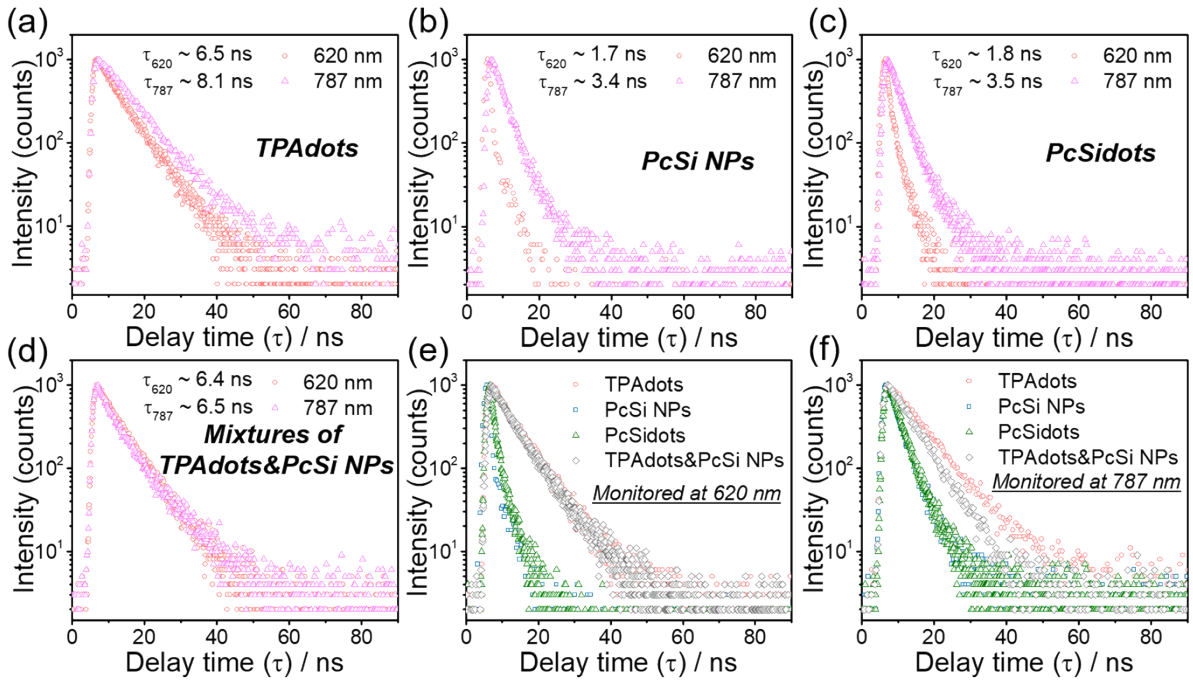

Figure S20. Fluorescence decays of TPAdots (a), PcSi NPs (b), PcSidots (c) and the mixtures of TPAdots&PcSi NPs (d, in the mixtures, $N_{TPA\text{-}BT}/N_{PcSi}$ = 200/1) in aqueous solution, monitored at 620 nm and 787 nm, respectively. Comparison of the fluorescence decays of TPAdots, PcSi NPs, PcSidots and TPAdots&PcSi NPs mixtures ($N_{TPA\text{-}BT}/N_{SQ}$ = 200/1) monitoried at 620 nm (e) and 787 nm (f). λ_{ex} = 375 nm.

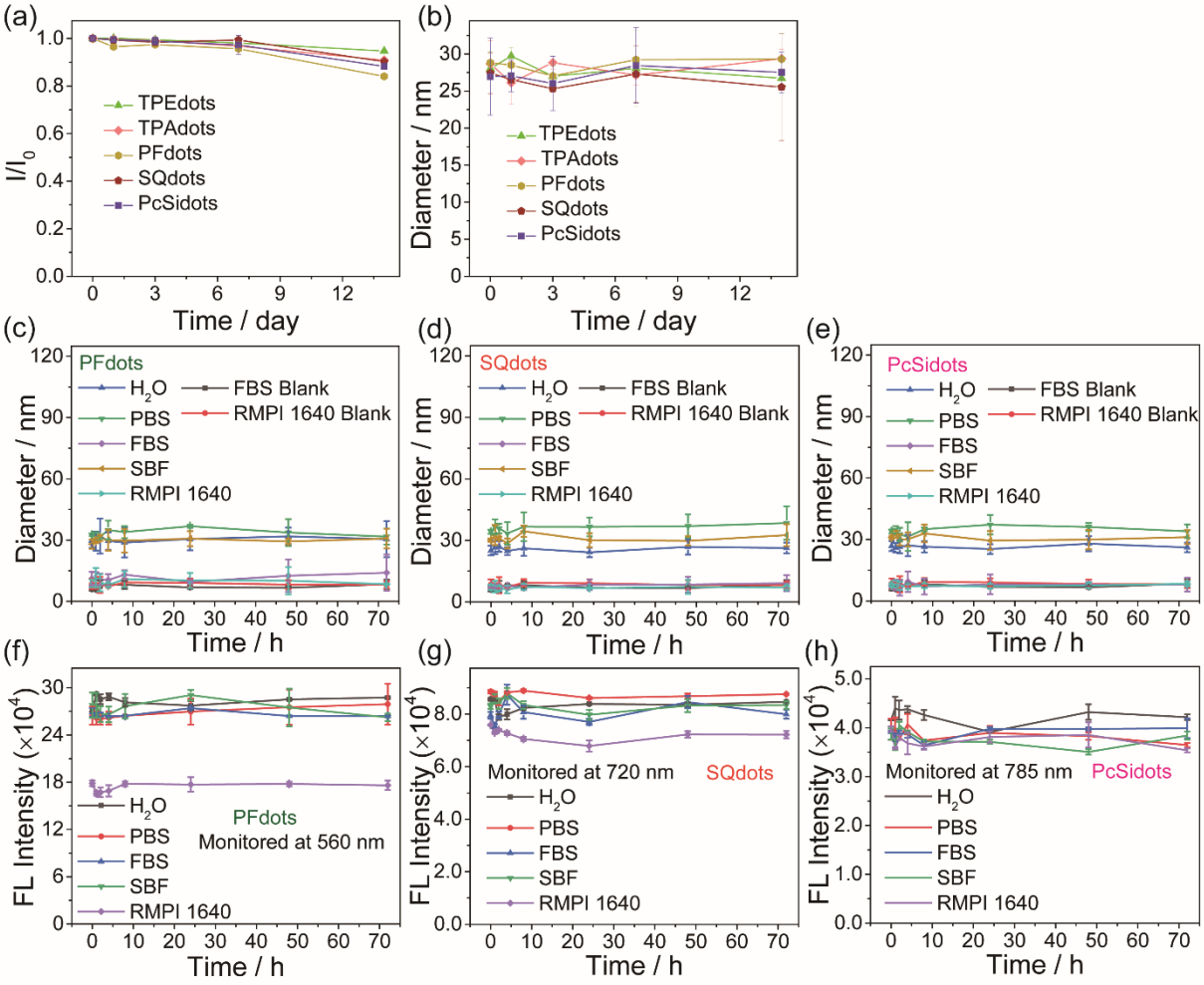

Figure S21. (a) Fluorescence intensity and (b) diameter measurement of the prepared AIEdots at different periods. Diameter characterizations and Fluorescence intensity of the prepared PFdots (c, f), SQdots (d, g), and PcSidots (e, h) dispersed in different mediums, respectively.

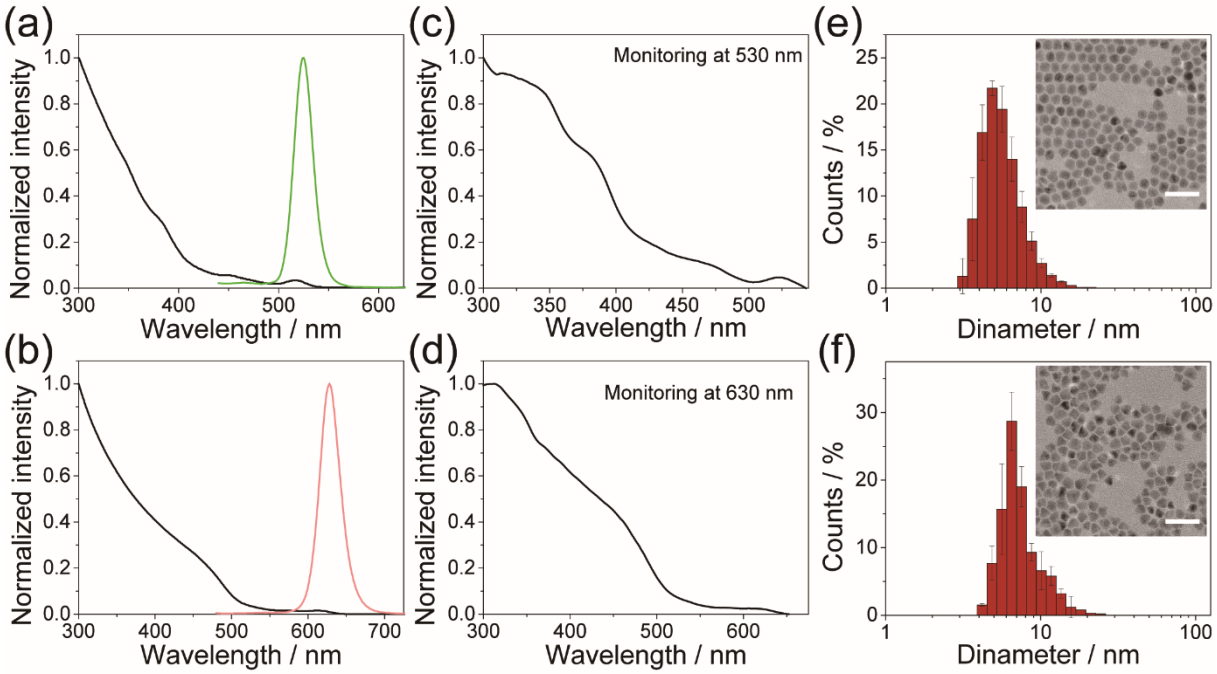

Figure S22. Absorption and fluorescence spectra of (a) QD525 and (b) QD625 in hexane. (c) Excitation spectra of QD525 in hexane at 530 nm. (d) Excitation spectra of QD625 in hexane at 630 nm. (e) DLS of QD525 in hexane, inset: TEM image of QD525. (f) DLS of QD625 in hexane, inset: TEM image of QD625. Scale bar: 20 nm.

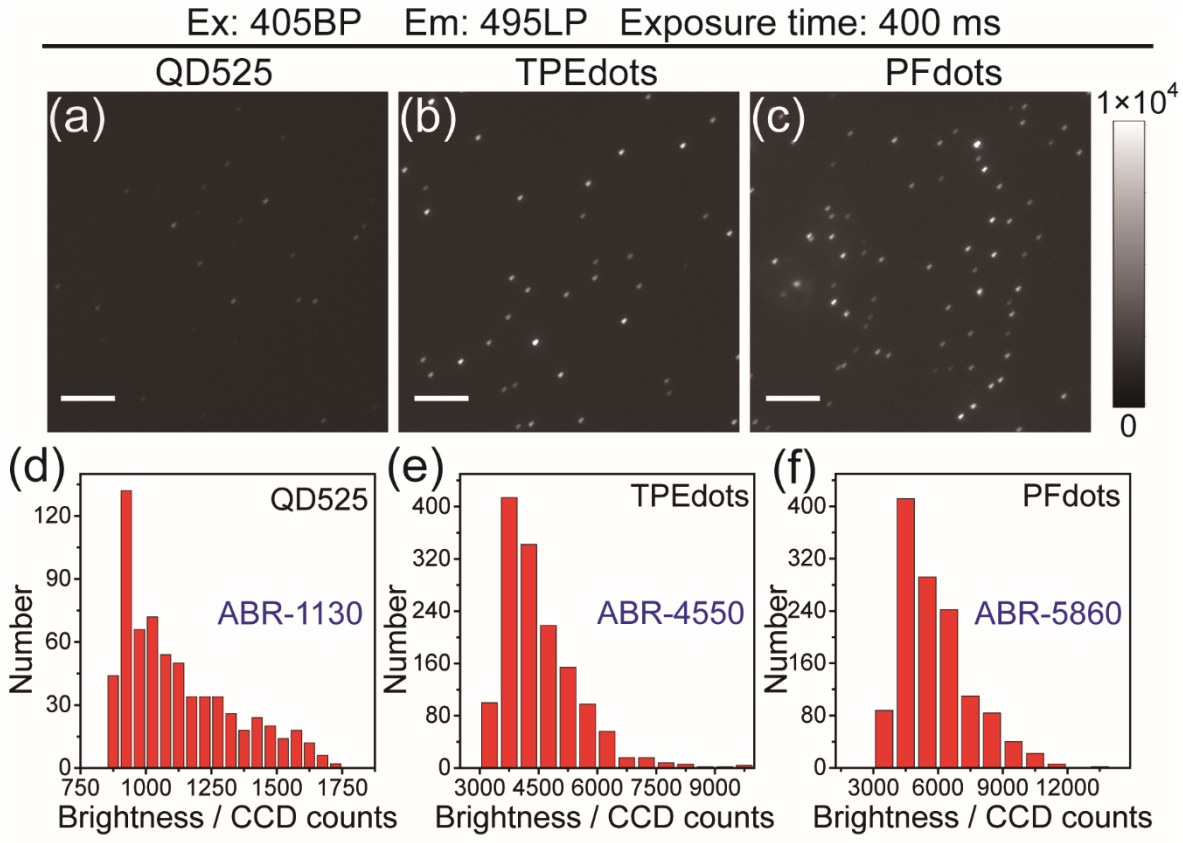

Figure S23. Single-particle fluorescence images of (a) QD525, (b) TPEdots and (c) PFdots, obtained with a xenon lamp using the same excitation (405BP) and collection condition (495LP, exposure time-400 ms). Scale bar: 5 μm. Histograms of the distributions of single-particle brightness of (d) QD525, (e) TPEdots and (f) PFdots.

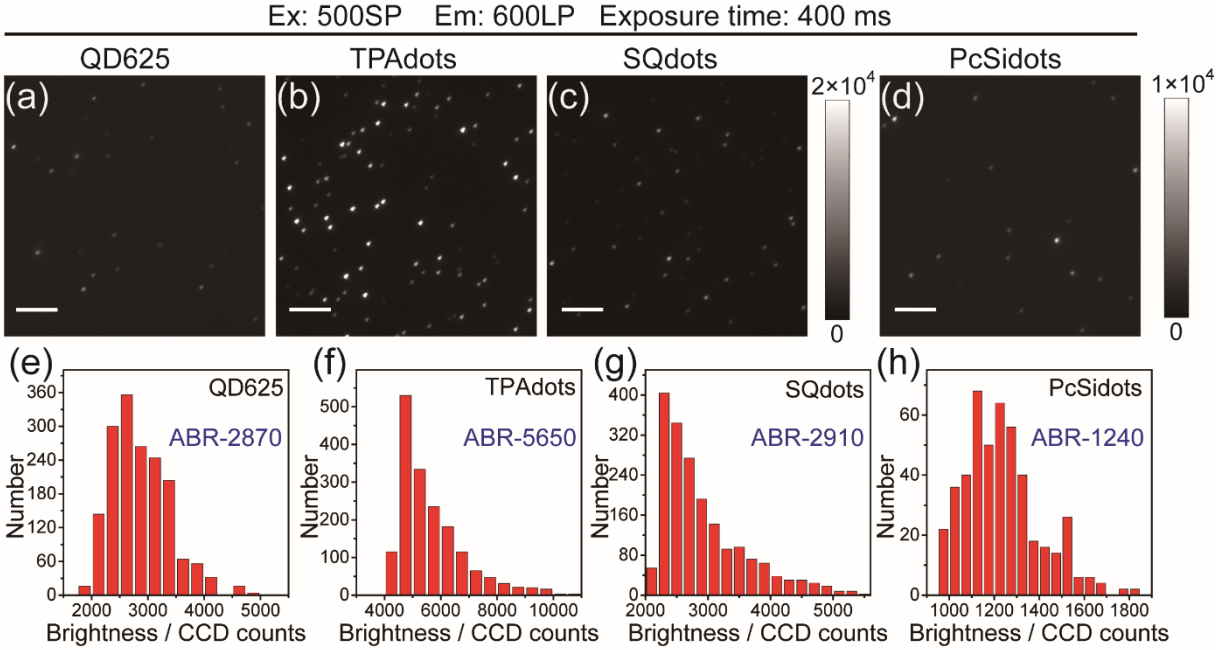

Figure S24. Single-particle fluorescence images of (a) QD625, (b) TPAdots, (c) SQdots and (d) PcSidots obtained with a xenon lamp using the same excitation (500SP) and collection condition (600LP, exposure time-400 ms). Scale bar: 5 μm. Histograms of the distributions of single-particle brightness of (e) QD625, (f) TPAdots, (g) SQdots and (h) PcSidots.

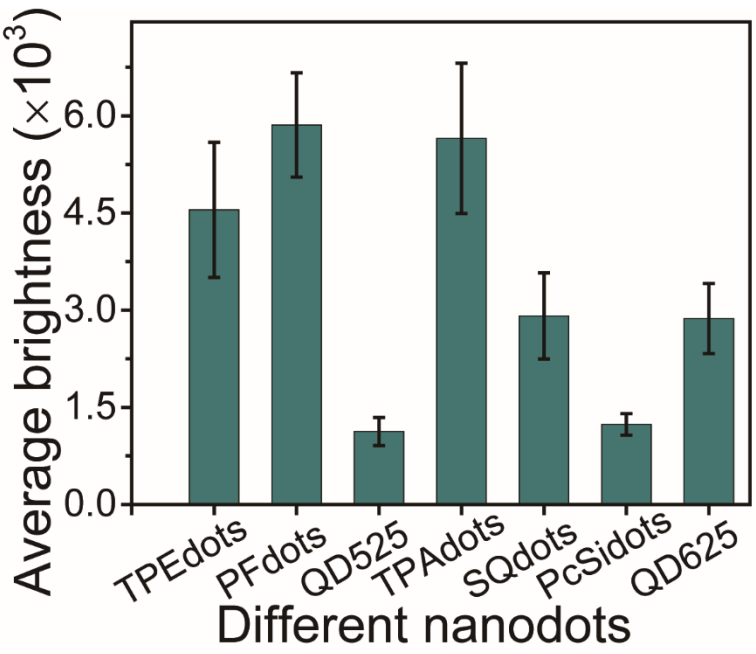

Figure S25. Average per-particle brightness of the prepared AIEdots and commerial QDs that shown in Figure S19 and Figure S20.

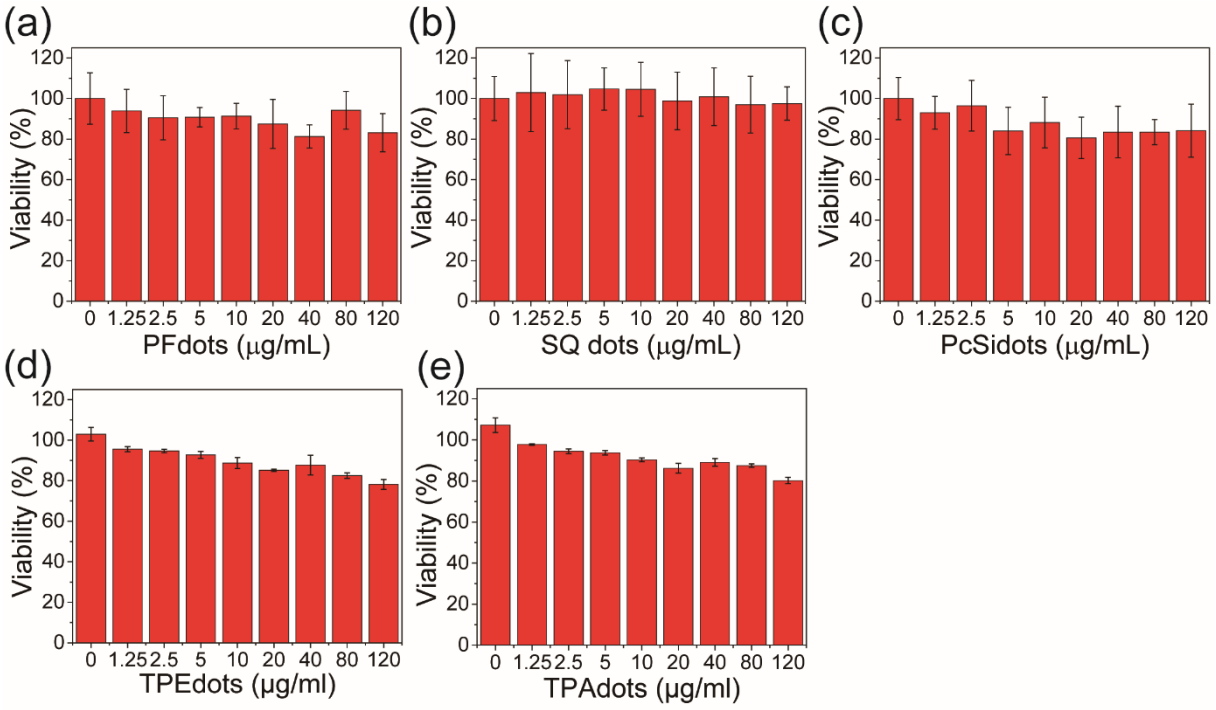

Figure S26. Cytotoxicity evaluation of **PFdots** (a), **SQdots,** (b) **PcSidots** (c), **TPEdots** (d) and **TPAdots** (e) over HeLa cell line.

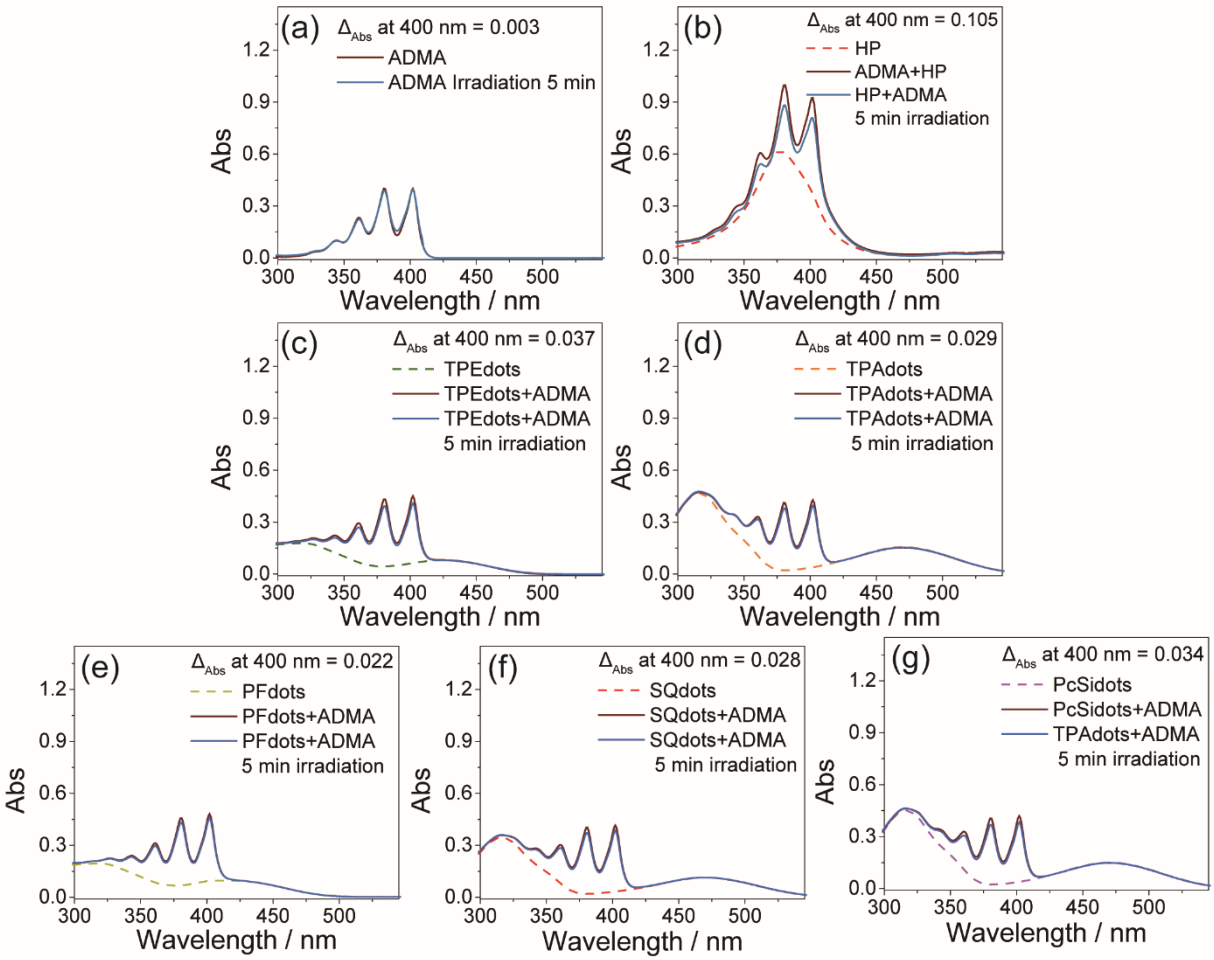

Figure S27. Measurement of photosensitized singlet oxygen ($^1O_2$) generation efficiency. Absorption spectra of single oxygen indicating probe ADMA (50 μM) recorded after 0 min and 5 min light irradiation in aqueous solutions containing buffer (a), hematoporphyrin (b), **TPEdots** (c), **TPAdots** (d), **PFdots** (e), **SQdots** (f) and **PcSidots** (g). The irradiation power is identical with the excitation condition applied in fluorescence imaging (xenon lamp equipped with 500 nm short-pass optical filter).

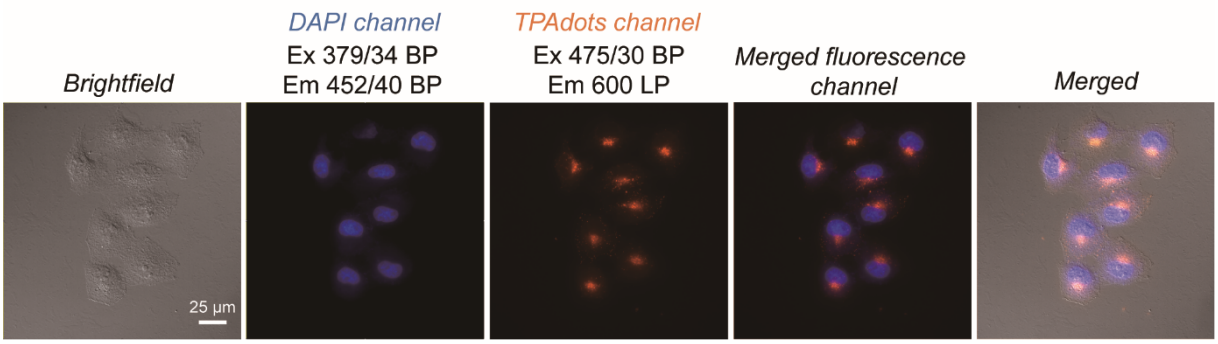

Figure S28. Co-localization of TPAdots and nucleus-located specific probe (DAPI). Bar: 25 μm.

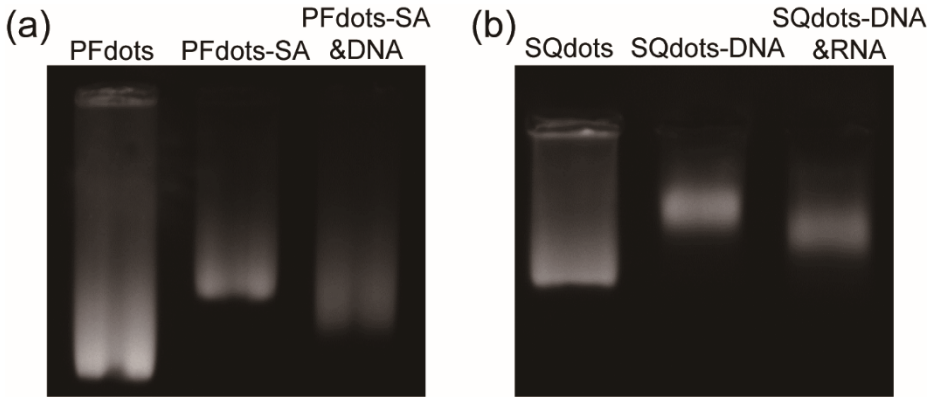

Figure S29. Gel electrophoresis of bare **PFdots**, streptavidin-conjugated PFdots and the mixture of PFdots-SA and DNA (a), bare **SQdots**, DNA-conjugated SQdots and the mixture of SQdots-DNA and RNA.

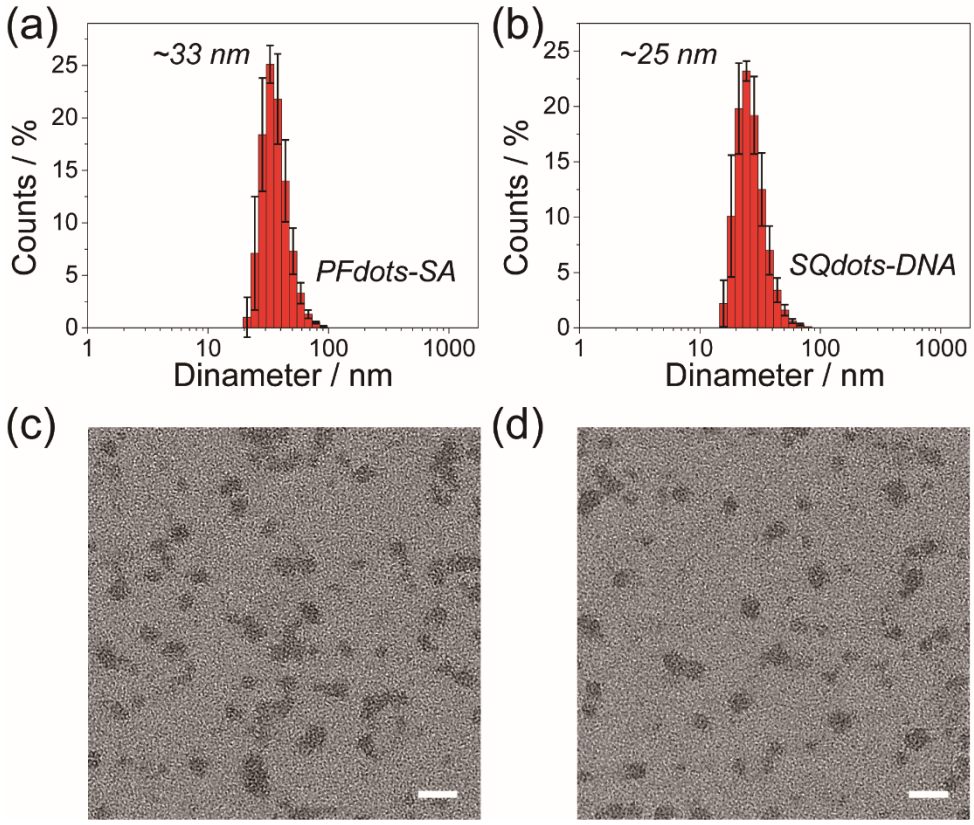

Figure S30. Histograms of size distribution measured by DLS for (a) PFdots-SA and (b) SQdots-DNA. TEM images of (c) PFdots-SA and (d) SQdots-DNA. Scale bar: 50 nm.

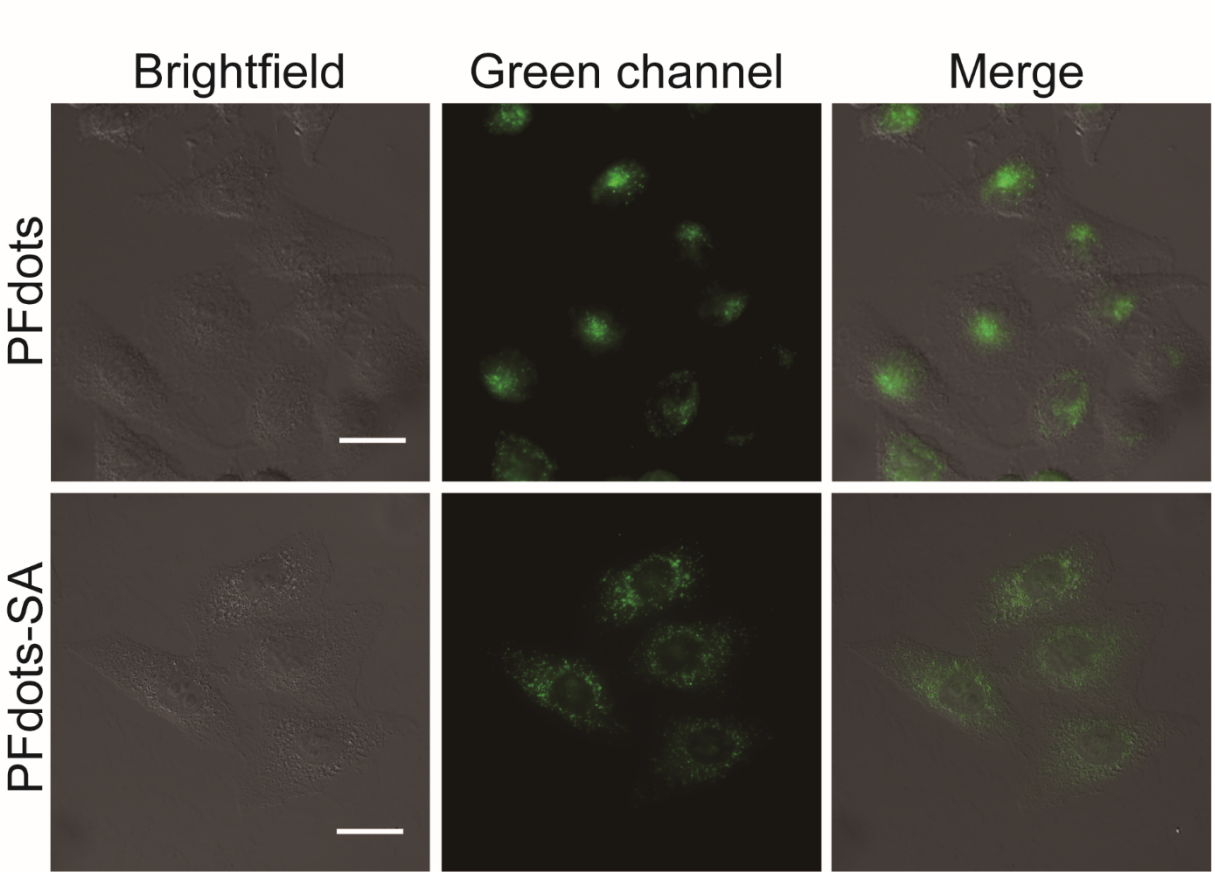

Figure S31. Fluorescence images of cells incubated for 24 h with PFdots and PFdots-SA (20 μg/mL). Excitation: xenon lamp, 500SP. Collection signal: 550BP. Scale bar: 25 μm

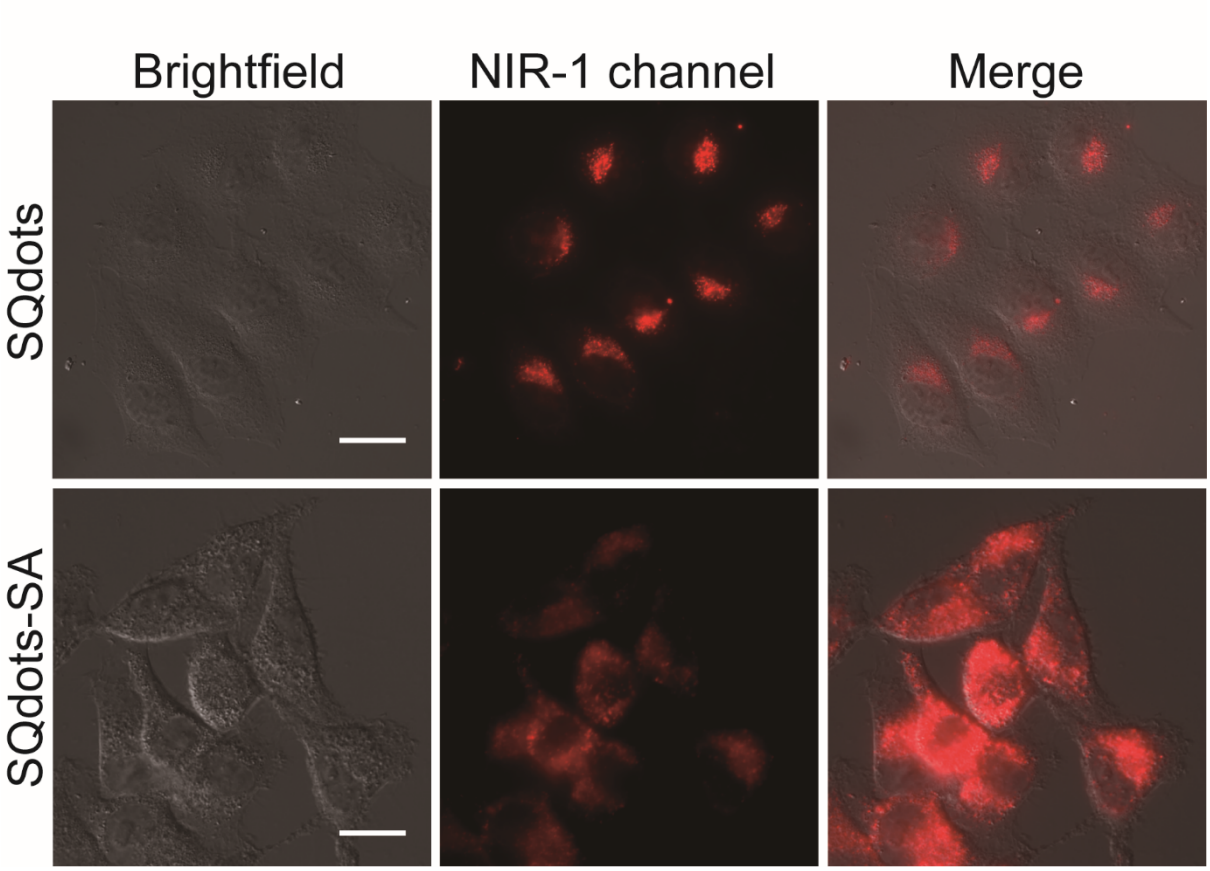

Figure S32. Fluorescence images of cells incubated for 24 h with SQdots and SQdots-DNA (20 μg/mL). Excitation: xenon lamp, 500SP. Collection signal: 732BP. Scale bar: 25 μm

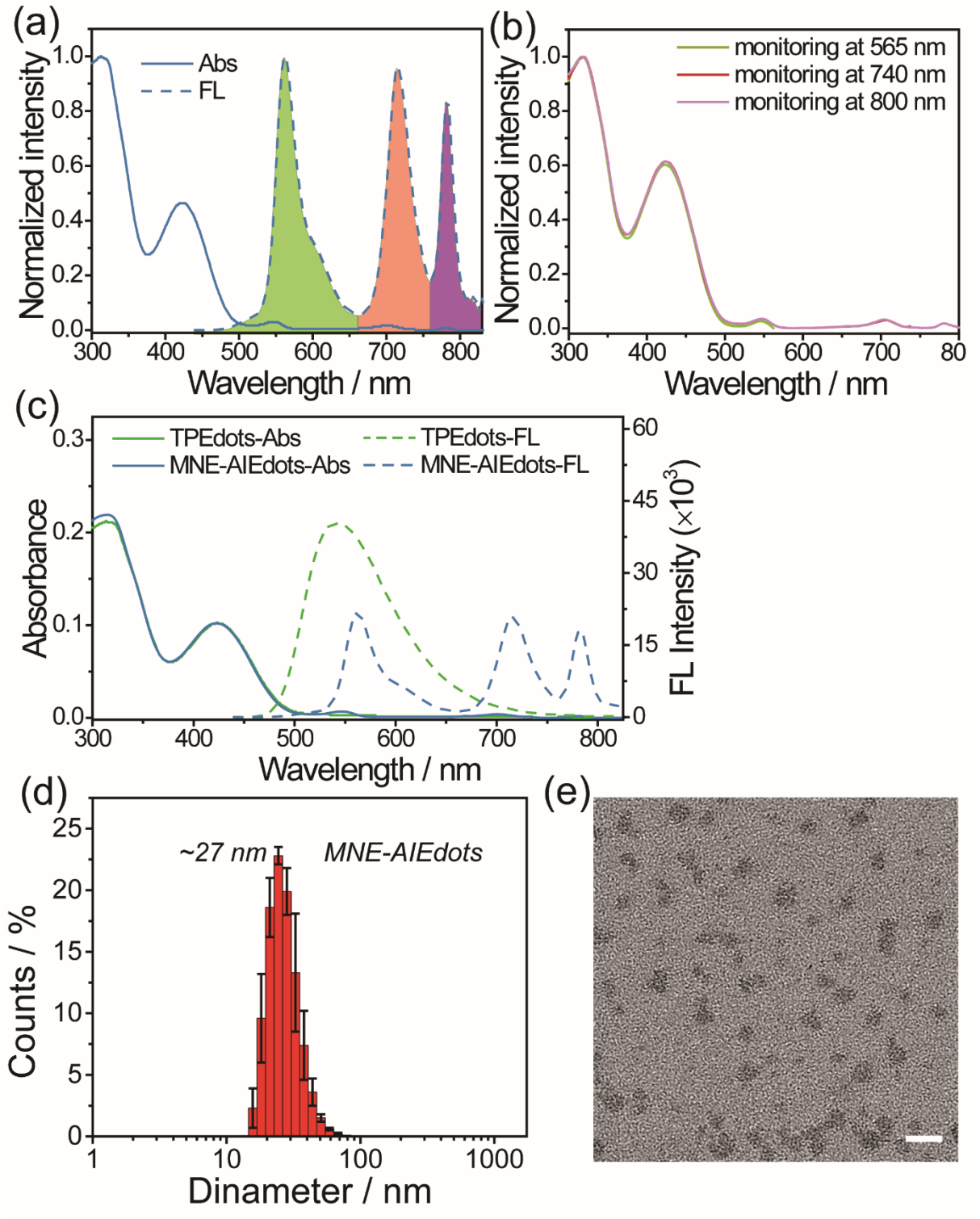

Figure S33. (a) Absorption and fluorescence spectrum of MNE-AIEdots. (b) Excitation spectra of MNE-AIEdots monitoring at 560 nm, 730 nm and 790 nm, respectively. (c) Absorption and fluorescence spectra of TPEdots and MNE-AIEdots with equal concentration. (d) Histograms of size distribution measured by DLS for MNE-AIEdots. (f) TEM image of MNE-AIE dots. Scale bar: 50 nm.

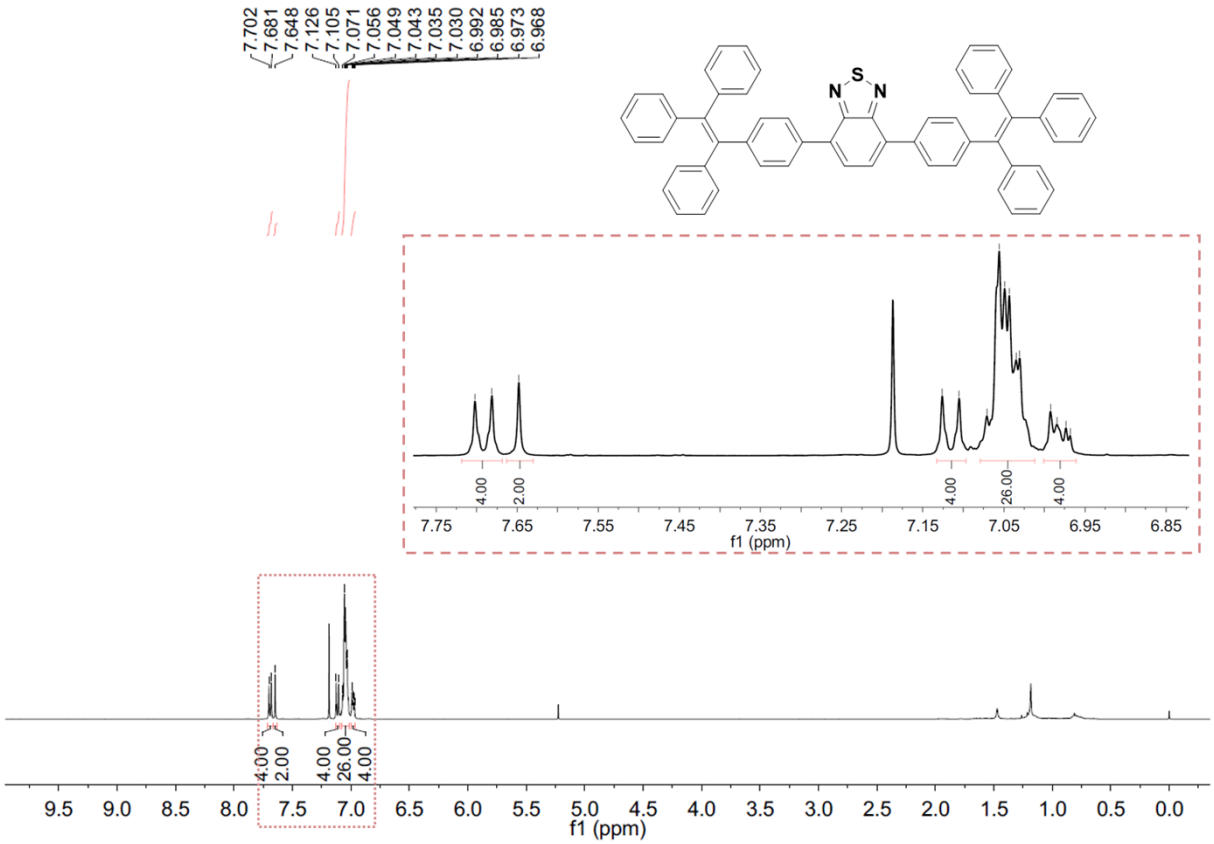

^{1}H NMR of TPE-BT ($CDCl_3$)

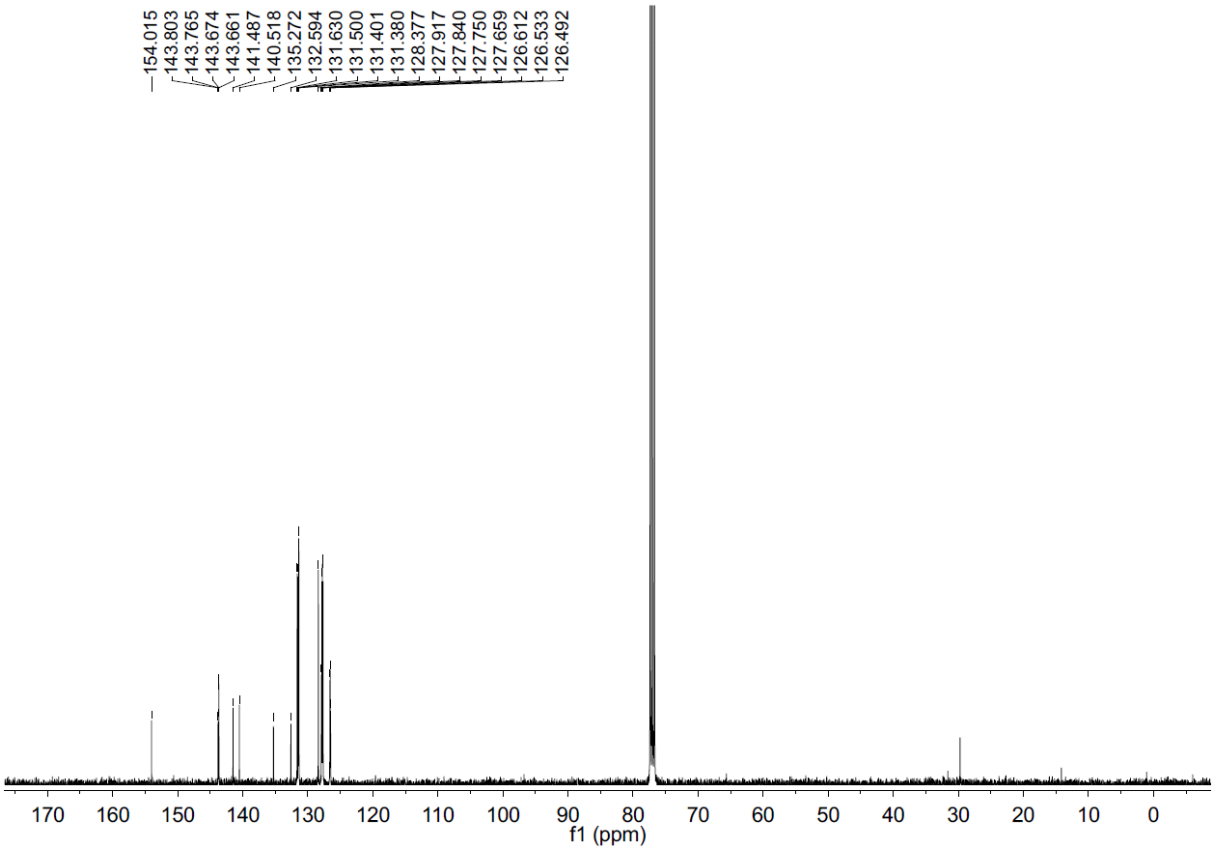

^{13}C NMR of TPE-BT ($CDCl_3$)

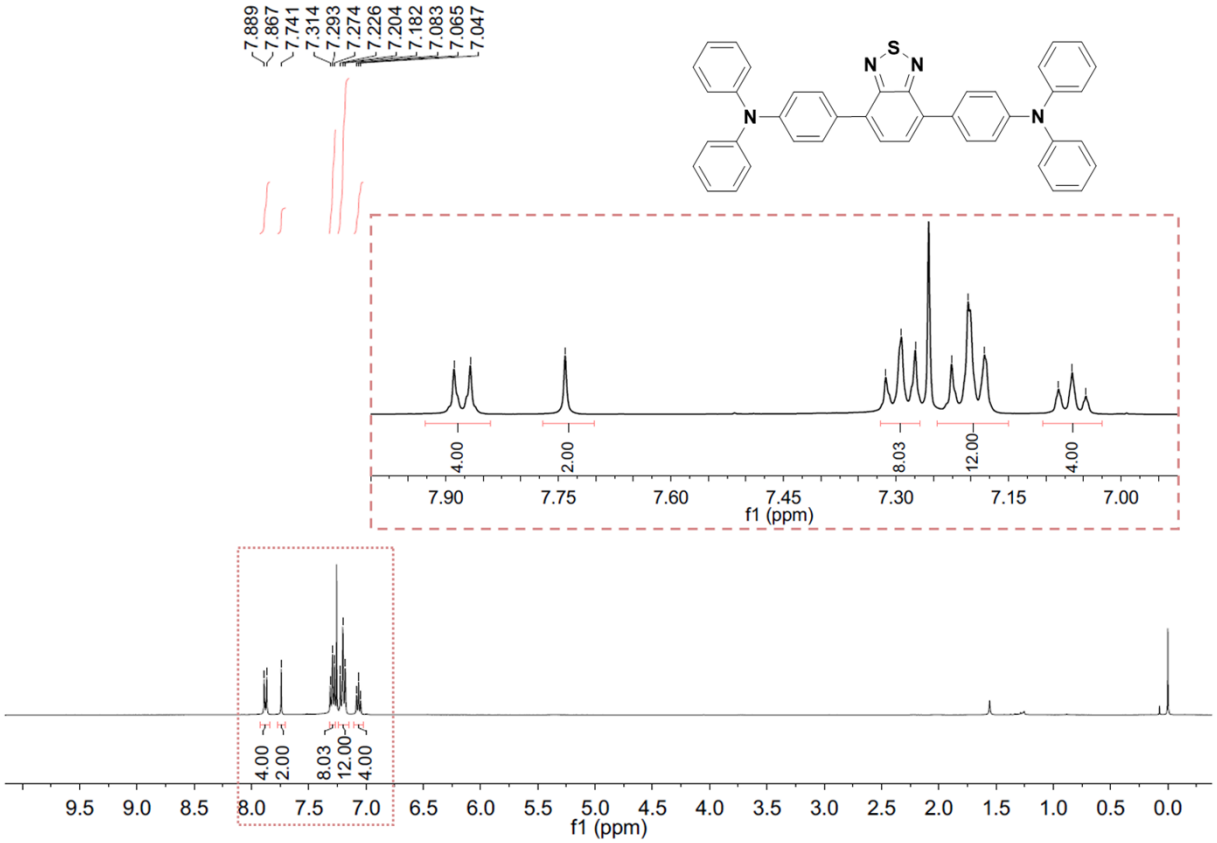

^{1}H NMR of TPA-BT($CDCl_3$)

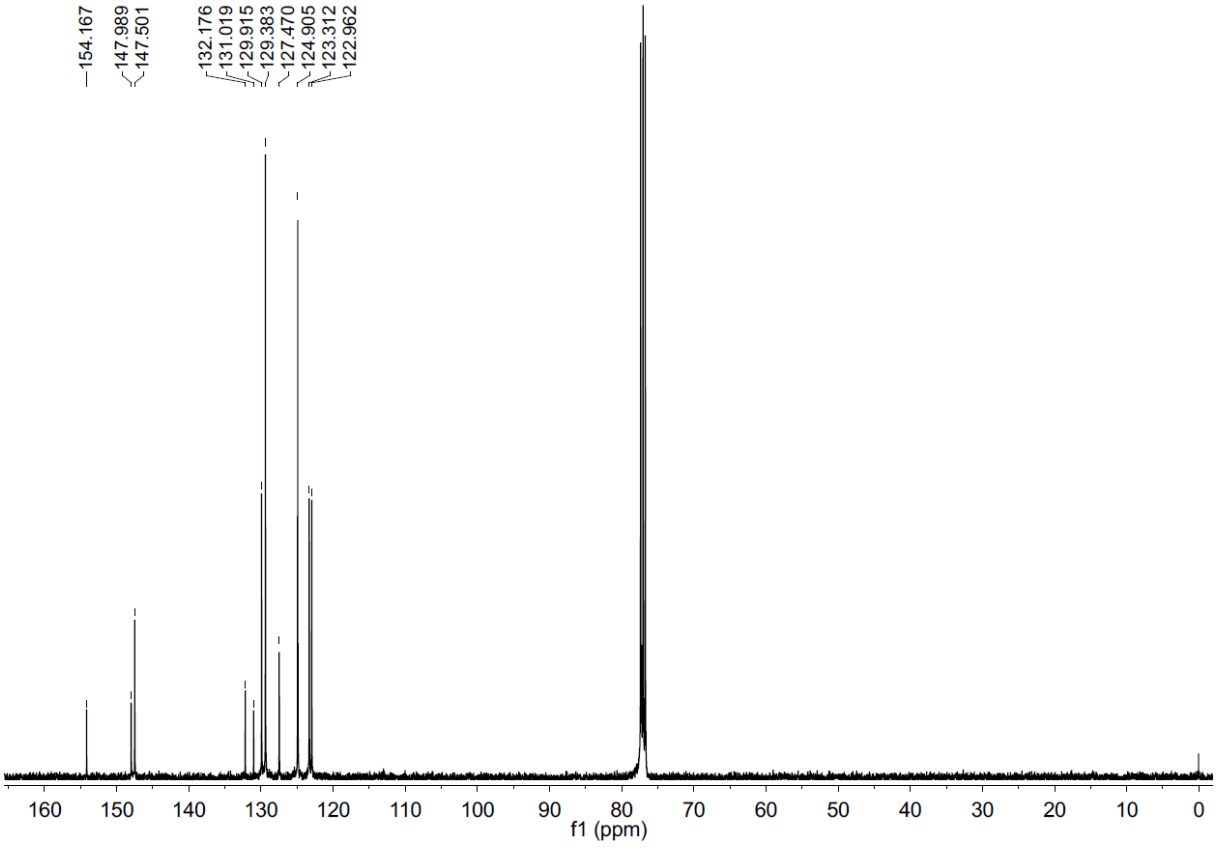

^{13}C NMR of TPA-BT ($CDCl_3$)

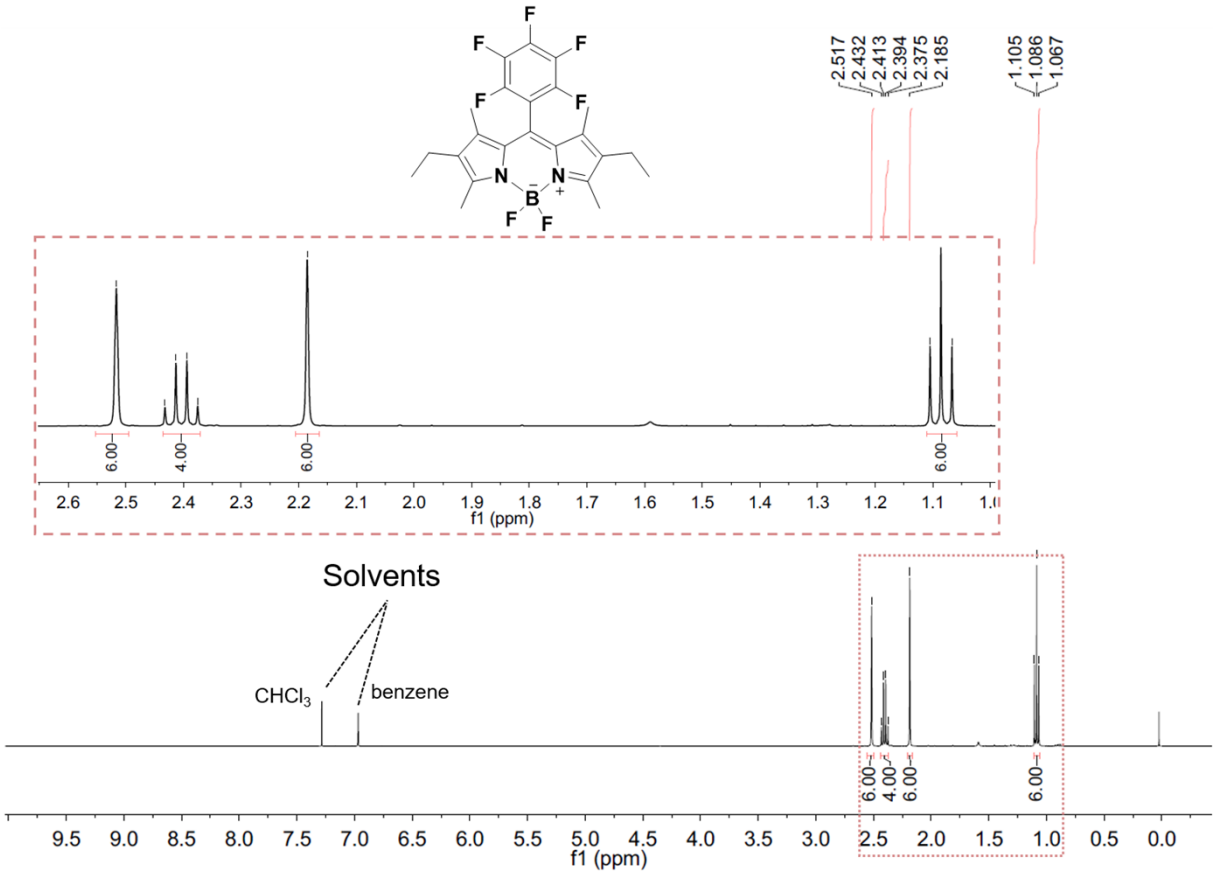

^{1}H NMR of PFBDP ($CDCl_3$)

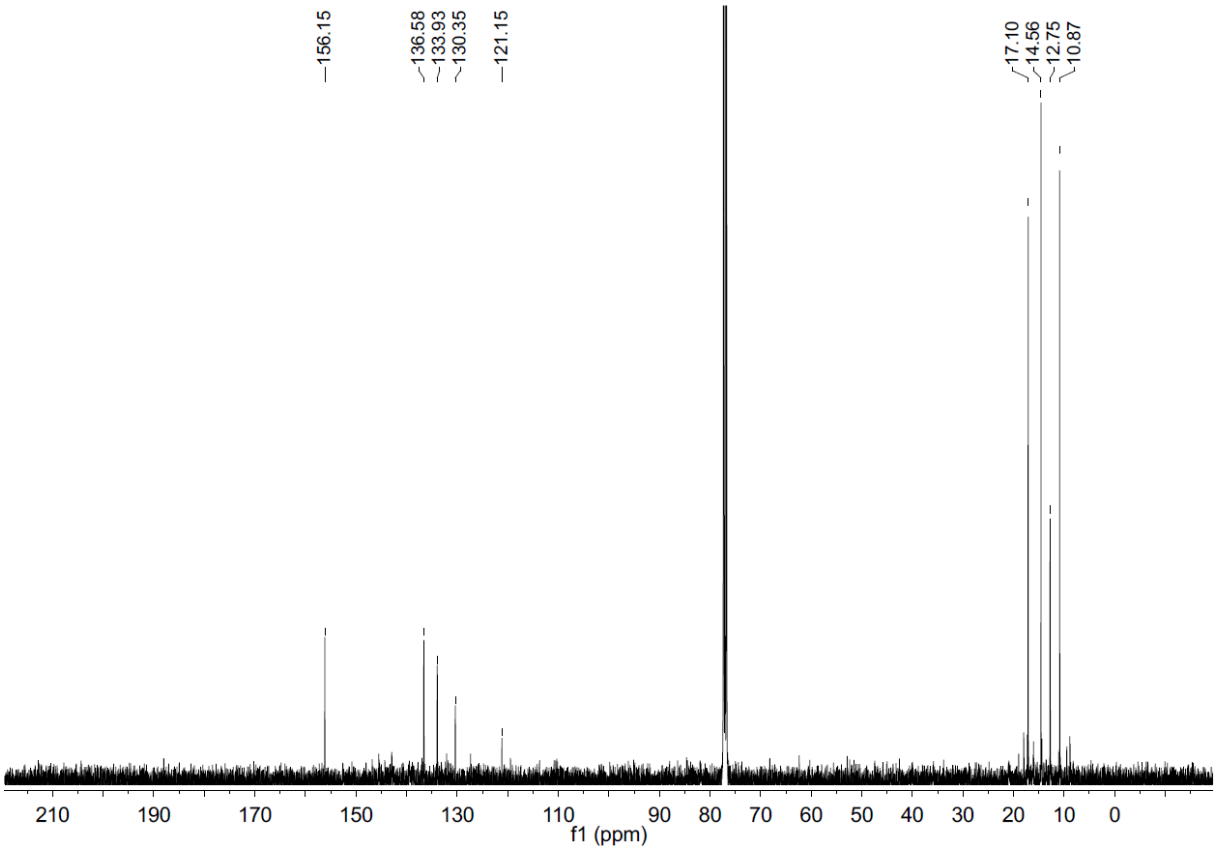

^{13}C NMR of PFBDP ($CDCl_3$)

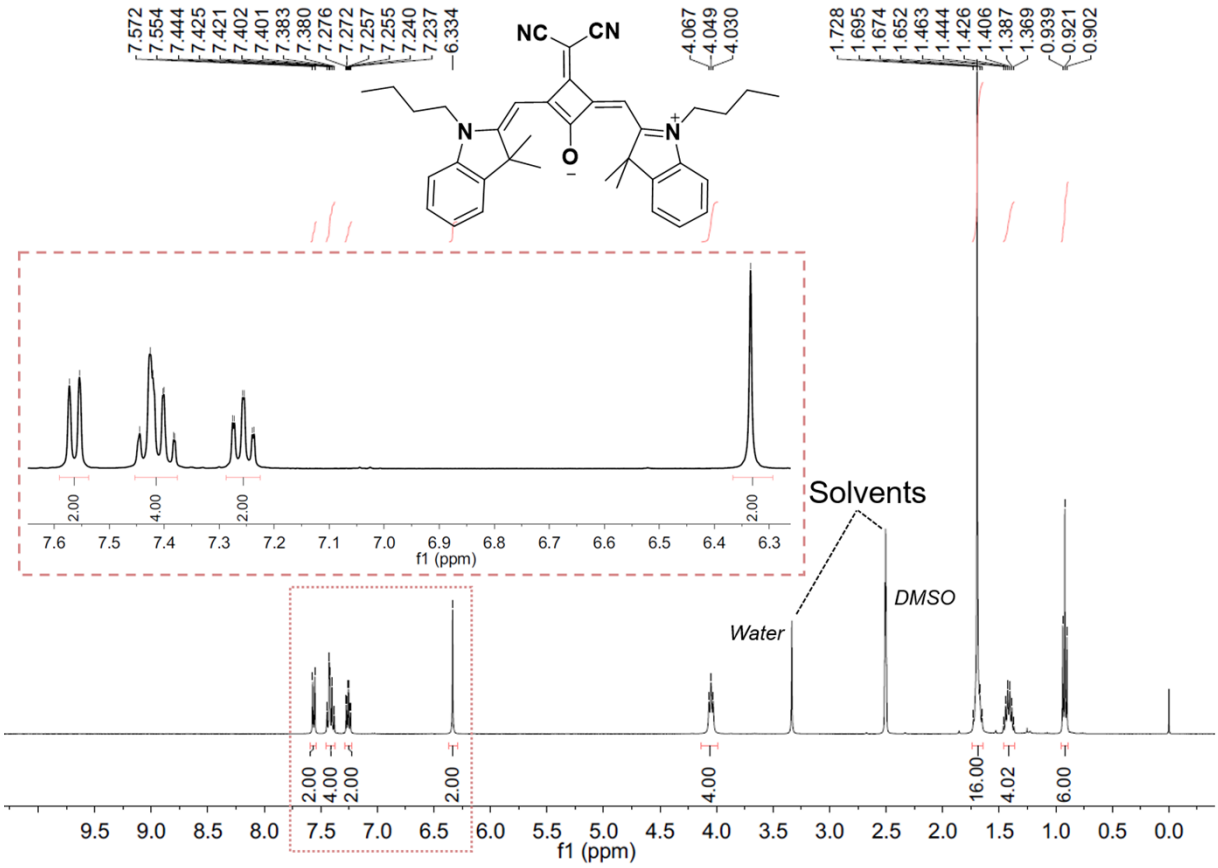

^{1}H NMR of SQ (DMSO-d$_6$)

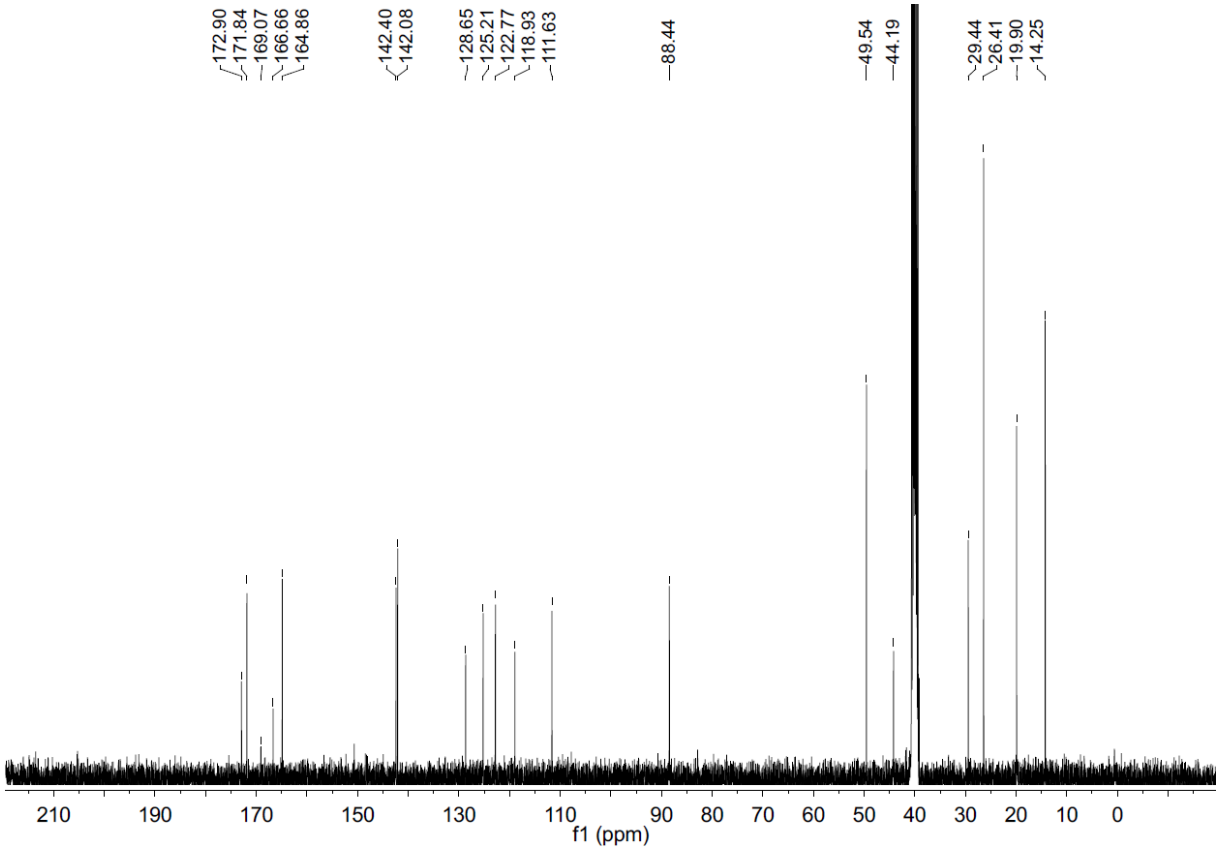

^{13}C NMR of SQ (DMSO-d$_6$)

Reference

[1] D. Ding, C. C. Goh, G. Feng, Z. Zhao, J. Liu, R. Liu, N. Tomczak, J. Geng, B. Z. Tang, L. G. Ng and B. Liu, *Adv. Mater.,* 2013, **25**, 6083-6088.

[2] S. Liu, H. Zhang, Y. Li, J. Liu, L. Du, M. Chen, R. T. K. Kwok, J. W. Y. Lam, D. L. Phillips and B. Z. Tang, *Angew. Chem. Int. Ed.,* 2018, **57**, 15189-15193.

[3] O. Galangau, C. Dumas-Verdes, R. Meallet-Renault and G. Clavier, *Org. Biomol. Chem.,* 2010, **8**, 4546-4553.

[4] U. Mayerhoffer, B. Fimmel and F. Wurthner, *Angew. Chem. Int. Ed.,* 2012, **51**, 164-167.

[5] J. W. Tian, L. Ding, H. J. Xu, Z. Shen, H. X. Ju, L. Jia, L. Bao, J. S. Yu, *J. Am. Chem. Soc.* **2013**, *135*, 18850-18858.